
Article:
Zhang, Y., Kumar, P. orcid.org/0000-0002-9965-8691, Lv, S. et al. (4 more authors) (2021) Recent advances in 3D bioprinting of vascularized tissues. Materials & Design, 199. 109398. ISSN 0264-1275

https://doi.org/10.1016/j.matdes.2020.109398

Materials and Design 199 (2021) 109398

Contents lists available at ScienceDirect

Materials and Design

journal homepage: www.elsevier.com/locate/matdes

Recent advances in 3D bioprinting of vascularized tissues

Yi Zhang [a,b], Piyush Kumar [b], Songwei Lv [a], Di Xiong [a], Hongbin Zhao [c], Zhiqiang Cai [a], Xiubo Zhao [a,b,*]

[a] School of Pharmacy, Changzhou University, Changzhou 213164, China
[b] Department of Chemical and Biological Engineering, University of Sheffield, Sheffield S1 3JD, UK
[c] Medical Research Centre, Changzhou Second People's Hospital Affiliated to Nanjing Medical University, Changzhou 213164, China

HIGHLIGHTS

- Introduction of the 3D bioprinting for tissue engineering applications.
- Overview of natural and synthetic polymers as bioinks for 3D bioprinting.
- Review of inkjet printing, extrusion-based printing, stereolithography, laser-assisted bioprinting technologies and their applications for the fabrication of vascularized tissues.
- Summary of challenges and future prospects of bioprinting for vascularized tissues.

GRAPHICAL ABSTRACT

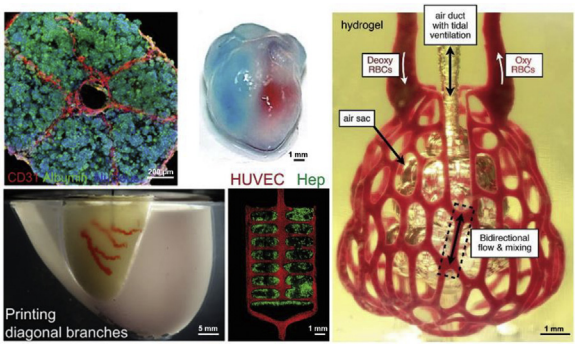

ARTICLE INFO

Article history:
Received 27 July 2020
Received in revised form 11 November 2020
Accepted 8 December 2020
Available online 10 December 2020

Keywords:
3D bioprinting
Bioink
Tissue engineering
Vascularized tissue
Inkjet bioprinting
Extrusion-based bioprinting
Stereolithography
Laser-assisted bioprinting

ABSTRACT

3D bioprinting is a technology that combines computing science, biology and material engineering. It has been extensively explored to fabricate 3D vascularized constructs for tissue engineering. This scalable, reproducible and highly precise fabrication technology offers great potential to achieve vascularization in printed tissues, which is an important milestone towards organ printing in the foreseeable future. A successful vascularized tissue integrates a range of hierarchical, perfusable channels within the mechanically supportive biomaterials. This review summarises the recent advances in the 3D bioprinting of vascularized tissues. Firstly, the common biomaterials used as bioinks for 3D bioprinting are introduced. While natural polymers are more suitable to mimic extracellular matrix resulting in effective cell growth, synthetic polymers offer tailorable mechanical properties and printability. Afterwards, the main 3D bioprinting techniques and their most recent practical applications in fabricating perfusable vascular networks are described. Furthermore, the future trends and prospects are also discussed.

Contents

* Corresponding author at: School of Pharmacy, Changzhou University, Changzhou 213164, China.
E-mail address: xiubo.zhao@sheffield.ac.uk (X. Zhao).

https://doi.org/10.1016/j.matdes.2020.109398

1. Introduction

3D printing was firstly introduced by Charles Hull in 1983 [1]. With the assistance of digital 3D computer aided design (CAD), the predesigned 3D structures at the desired scale can be precisely fabricated in a bottom-up and layer-by-layer manner. As 3D printing offers great geometric accuracy, it has found extensive applications in the fabrication of 3D structures with complex internal architecture and unique external features without employing excessive tooling which can incur high manufacturing costs, wastage of valuable time and inefficiency of human resources. These applications include a wide range of areas such as aerospace engineering [2,3], automotive industries [4,5], electronics manufacturing [6–8], tissue engineering [9–18], regenerative medicine [19–21], food industries [22–24], drug delivery [25–28], cancer research [29–33], high-throughput screening tests [34–36], self-propelled microdevices [37–39], joint replacement implants [40–42], prosthetics [43,44] and bio-robot models [45].

3D bioprinting is the process that patterns and assembles living and non-living biomaterials via a 3D structural organization using computer-aided transfer processes [46–48]. Because of its superior precision, fast production and easy manipulation, bioprinting has been intensively explored for fabricating cell-laden tissue scaffolds for tissue engineering with the ultimate goal of organ printing [49–57]. Traditionally, the replacement of defected tissues/organs relies on transfer of the autologous and allogeneic ones. However, the extreme lack of donors is the main limitation which delays the effective treatment for patients [58]. To address this issue, bioprinted tissues/organs with tissue-specific cells and customized sizes can be the promising substitutes for the autologous/allogeneic treatment [59]. The advantage of using 3D bioprinting to fabricate tissues/organs is the flexibility of using different biomaterials and specific cells and, thus, a multi-scale and multi-material fabrication process can be achieved [60]. By simultaneously printing biocompatible materials as matrices, tissue-specific cells and bioactive growth factors, following a predesigned order of different layers, the printed 3D constructs can promote tissue regeneration and restore their functions effectively [61–63].

Natural vascular tissues/organs have a range of vessel networks with different structures and size range from micrometre-sized capillaries to millimetre-sized vessels [64,65]. Capillaries have a monolayer of endothelial cells (ECs) while larger vessels have three layers: (1) an inner EC layer; (2) a middle layer which is composed of smooth muscle cells (SMCs), elastic tissue and collagen fibres; (3) an outer layer which is composed of elastic tissue and collagen fibres [66]. Moreover, different sized vessels have different types of ECs, and the following three types of ECs are commonly used in tissue engineering applications: human umbilical vein endothelial cells (HUVECs), human microvascular endothelial cells (HMVECs), and induced pluripotent stem cell-derived endothelial cells (iPSC-ECs) [66]. Amongst them, HUVECs are the most frequently used endothelial cell type for bioprinting vessels. HMVECs have great potential to form microvascular networks as they are originally obtained from micro-vessels. As iPSCs are capable of self-renewal and multi-lineage differentiation, ECs derived from iPSCs are an ideal autologous alternative to primary ECs [67]. Additionally, as human iPSCs (hiPSCs) reprogrammed from patients' specific cells do not cause immunological response, the hiPSC-ECs have gained extensive attention for 3D bioprinting of customized vascularized tissues/organs [68–70]. On the other hand, SMCs play an important role in vessel structure and function in physiological and pathological conditions.

In terms of vessel formation, vasculogenesis and angiogenesis are the two most studied models. Vasculogenesis triggers the formation of primitive vascular plexus during embryonic development. It also happens in the process of EC differentiation from endothelial progenitor cells. Angiogenesis is the process in which ECs sprout and form new blood vessels from pre-existing vessels. It normally has two stages: sprouting and intussusception. Sprouting needs the assistance of growth factors such as vascular endothelial growth factor (VEGF), angiopoietin-2 (Ang2), and fibroblast growth factor (FGF) to trigger the proangiogenic gene in quiescent vessels to form interstitial columns/tubes. Intussusception is the process in which the interstitial cellular columns are inserted into the pre-existing vessels followed by the growth of those columns to form new vessels [66].

Although current 3D bioprinting has achieved a remarkable breakthrough in fabricating a small range of vascular networks *in vitro*, there is still a gap between clinically implantable vascularized tissues/organs and the capabilities of the current techniques. One of the vital challenges of 3D bioprinting of vascularized tissues is to create a range of hierarchical and perfusable channels with specifically allocated biomaterials and cells to allow the access of cells to nutrients and oxygen, and removal of wastes [71–75]. Lack of suitable vasculature in the bioprinted tissues has limited its applications in the area of tissue regeneration [76,77]. Manufacturing of personalised tissues/organs would be the ultimate goal of 3D bioprinting, as patients can be treated more efficiently and effectively by transplanting customised tissues/organs instead of the allogeneic ones [78]. Overall, a successful 3D bioprinted tissue should have the following typical characteristics: (1) replicate the tissue-specific vascular networks in a certain size range; (2) possess sufficient mechanical properties which match the host tissue; (3) integrate with the body vascularization system to maintain tissue functions.

This review summarises the recent advances in the 3D bioprinting of vascularized tissues. The commonly used biomaterials, 3D bioprinting techniques and their most recent practical applications in fabricating perfusable channels/vascularized constructs are described. Furthermore, the future trends and prospects are also discussed.

2. Biomaterials used in vascular bioprinting

Biomaterials and cells are the most important components used in vascular bioprinting. It has recently been defined by Groll et al. [79] that a 'bioink' is a formulation of cells that may also contain biologically active components and biomaterials and is suitable for processing by an automated biofabrication technology. On the other hand, a formulation containing only biomaterials and/or bioactive components was defined as 'biomaterial inks' [79]. The ideal biomaterials used in bioinks or biomaterial inks for fabricating vascularized tissue should not only be capable of forming 3D structures with high resolution, appropriate mechanical properties and biodegradability to act as a supportive frame, but also possess good biocompatibility and low cytotoxicity to facilitate cell growth. Natural polymers such as fibrin, collagen, gelatin and alginate possess excellent biocompatibility which allows them to be commonly formulated with cells to form bioinks. Besides, they are suitable to mimic extracellular matrix (ECM) environment, leading to effective cellular growth and function, hence resulting in effective tissue regeneration. However, these biomaterials usually encapsulate and confine cells, which results in limited cell-to-cell interactions [80]. Furthermore, natural polymers commonly have poor mechanical properties and undesirable fast degradation rates which limit their applications in bioprinting. Therefore, synthetic polymers have been increasingly used or combined with natural biomaterials to print 3D constructs for tissue engineering as they can offer excellent mechanical property to match the loading requirements of native tissues or organs. Moreover, synthetic polymers have tailorable processability which is beneficial to the resolution of 3D bioprinting [81]. Therefore, composite materials composed of both synthetic polymers and natural biomaterials are the best promising candidates for 3D bioprinting in the future.

2.1. Natural polymers

2.1.1. Collagen

Collagen is the main component of ECM which makes it an excellent candidate for supporting cell growth for tissue regeneration. Type I collagen hydrogels are the most frequently used collagen protein type for 3D printing of vascularized tissues as they provide an ideal microenvironment for angiogenesis. In order to facilitate the formation of specific vasculature, the concentration of collagen needs to be carefully selected. Collagen gels with concentrations between 1.2 to 1.9 mg/mL support stable sprout formation as they allow the EC proliferation and migration [82]. Collagen has been primarily used for extrusion-based bioprinting as it offers quick gelation rate under suitable conditions and acceptable mechanical properties after gelation. The gelation kinetics of collagen hydrogels are dependent on pH and temperature, with a maximum storage modulus recorded at pH 8 and 37 °C, respectively [83]. However, lack of sufficient mechanical properties is the main limitation of applying collagen-only hydrogels as load-bearing tissue scaffolds [84]. Therefore, synthetic polymers with better mechanical properties were combined with collagen to support the structure of the final constructs.

In order to improve the printability of collagen gels, biocompatible and non-toxic crosslinkers, such as tannic acid, can be adopted [85]. With the assistance of crosslinker, a 3D structure of intestinal villi with an endogenous capillary network has been reported recently [86]. In addition to a suitable crosslinker, materials with relatively fast gelation rate can be blended with collagen to optimise the printability of collagen hydrogels. Alginate has been used for blending with collagen to accelerate the gelation process and achieve a better shape fidelity. After gelation, alginate was removed from the structure by chelation, leaving a collagen-only 3D structure. Although collagen has been promisingly used for 3D bioprinting, its inferior printability hinders its application for printing vessels with high resolution. Other than blending with different materials to improve the printing resolution of collagen-based hydrogels, using suitable printing techniques may be another solution to address this issue.

2.1.2. Gelatin

Gelatin is a fibrous protein derived from collagen by irreversible hydrolysis. Gelatin has the advantages of high water-absorbing ability, excellent biocompatibility, non-immunogenicity and complete biodegradability. Aqueous gelatin is thermosensitive and forms hydrogel through hydrogen bonding at low temperatures (< 35 °C), whereas at 37 °C, the solid gelatin can turn into viscous liquid and easily be printed using extrusion-based printing. As pure gelatin dissolves completely within 24 hrs, it is usually used as a sacrificial support material which is removed after printing, leaving hollow channels for obtaining vascularized tissues. As mentioned above, as HUVECs are the main endothelial cell type used to form vessels. HUVEC-laden sacrificial gelatin bioink has been increasingly used to fabricate vascularized tissues. After removing gelatin from the matrix, which is usually collagen, the inner surfaces of the hollowed channels get lined with HUVECs which promote the vessel formation by angiogenesis. Although researchers have endeavoured to improve the printability and stability of gelatin-based bioinks, for example, by using thickeners (e.g. nanoclay) and transglutaminase to increase the shape fidelity of final gelatin 3D structures [87,88], low printing resolution (> 100 μm) is the main obstacle in using gelatin-based bioinks as matrix materials for 3D bioprinting.

To address this issue, gelatin has been methacrylated which can be covalently cross-linked to form a stronger material (i.e. GelMA) with decent biological and physicochemical properties for 3D bioprinting. GelMA has excellent processability and can be reversibly crosslinked by heat and irreversibly stabilized by UV [89,90]. Moreover, the physicochemical properties of final products can be tuned by crosslinking density of methacryloyl group. Therefore, GelMA is a promising biomaterial that can preserve the integrity of the final bioprinted constructs and maintain a good cell viability, proliferation and spreading for 3D bioprinting of vasculature [91]. In order to directly print perfusable channels, GelMA has been increasingly combined with alginate for coaxial extrusion-based printing. With the assistance of rapid-gelling alginate, the shape fidelity of the coaxially printed tube can be well preserved. Again, ECs, such as HUVECs, and growth factors, such as VEGF, can be blended into those bioinks to form vessels in the final structures with good cell viability. Additionally, the mechanical properties of GelMA-based hydrogels can be tuned according to the requirement of specific tissues. Soft GelMA-based hydrogels promote vasculogenesis and capillary formation of human dermal microvascular ECs, while stiffer GelMA-based hydrogels support osteogenesis and bone formation. The main disadvantage of using GelMA as matrix material for bioprinting is the UV-dependent gelation process. UV exposure and toxic photoinitiators have been reported that negatively affect cell-viability. Therefore, crosslinking using blue light (405 nm) is more preferred.

2.1.3. Decellularized extracellular matrix

Decellularized extracellular matrix (dECM) is the cell-removed tissue which retains the ECM frameworks. As ECM is a mixture of different components, such as collagen, elastin and growth factors, dECM is a cell-friendly material which offers excellent biological activity, easy processability and tailorable degradation rates [92,93]. These advantages make dECM a promising candidate for 3D bioprinting of vascularized tissues without an excessive number of steps for blending different ingredients. Moreover, as each tissue or organ has its specific ECM components, using dECM of targeted tissue offers better cellular growth and function than using other biomaterials [94]. Additionally, to match the stiffnesses of different tissues, the mechanical properties of printed dECM constructs can be tailored by incorporating crosslinkers such as PEG-based crosslinkers or methacrylating dECM to make it UV-crosslinkable [95,96]. As the components of different tissues support different biological functions, it is ideal to use dECM which is derived from natural vascular tissues, such as ethically derived aorta and *venae cavae*, as the biomaterial for bioprinting of vascularized tissues. Furthermore, considering the potential immune response and accidental pathogen transfer

induced from the non-autologous dECM, it is ideal to use patient-specific tissue derived dECM as the biomaterial for printing vascularized tissues [97,98].

However, a relatively slow gelation process hinders the use of dECM for 3D bioprinting as the shape fidelity is poorly preserved. This disadvantage can be improved by incorporating fast-gelling materials such as alginate. Furthermore, making dECM UV-crosslinkable provides the potential to use laser-assisted printing techniques to increase the printing resolution of the final 3D structures.

2.1.4. Fibrin

Fibrin is the main extracellular constituent of blood clot and possesses inherent cell-adhesion capabilities on account of its multiple cell-adhering motifs [99,100]. Fibrin helps EC proliferation by directing associated cells to growth factors, such as VEGF and FGF, to promote angiogenesis [101,102]. Fibrin also supports the growth of ECs as a scaffolding material and exhibits shear-stiffening property under high strains, which can mimic the non-linear elastic behaviour of soft tissues. Therefore, fibrin has been widely used for wound healing and tissue remodelling [103–105].

However, lack of decent mechanical property and rapid degradation are the main limitations of using fibrin as a 3D bioprinting material. Therefore, blending fibrin with more printable polymers to make mechanical property and degradability more tunable could be a solution to address this issue. Another possible option is to chemically modify fibrin, for example, by conjugating fibrin with PEG to better control the mechanical properties while maintaining good bioactivity of fibrin.

2.1.5. Alginate

Alginate, which is renewably sourced from brown algae, forms hydrogel through ionic crosslinking in the presence of divalent cations, such as Ca^{2+}, Mg^{2+} and Ba^{2+}. The cross-linked alginate hydrogel is composed of hydrophilic polymer chains which have a large water-holding capacity. Moreover, its porous internal structure plays an important role in the diffusion of nutrients and gases for cellular metabolism and removal of the resultant wastes. Therefore, alginate hydrogel has been widely used as scaffolding material for tissue engineering. As alginate possesses rapid gelation capability, which improves the shape fidelity, tailored degradability and shear-thinning characteristic which minimises the effect of shear stress on cells, it has been extensively used in inkjet and extrusion-based 3D bioprinting [91,106]. For inkjet printing, the viscosity of inks is mainly affected by concentration and molecular weight of alginate, cell density and temperature, with too viscous inks (> 20 mPa s) being not able to be jetted out [107]. Pre-crosslinking is usually applied before extrusion-based printing to provide sufficient deposition quality followed by exposing the printed scaffolds to high concentration crosslinker to achieve full crosslinking. In addition to being a matrix material, alginate has also been used as a sacrificial material to help achieve a high shape fidelity in perfusable tubular structures [108]. The removal of the ionically cross-linked alginate hydrogels from a construct can be achieved by releasing the divalent ions crosslinkers via exchange reactions with monovalent cations present in the surrounding medium [109].

Although ECs have been incorporated with alginate to form bioinks for 3D bioprinting of vascularized tissues, the viability of ECs in alginate hydrogels was only around 71% with alginate hydrogels not supporting vascular morphogenesis, which is not ideal compared to that of other aforementioned biomaterials [110]. In order to improve its biocompatibility and bioactivity, incorporating more cell-friendly biomaterials, such as collagen and fibrin, and/or proangiogenic growth factors, such as VEGF, have been approved as good approaches to facilitate the vascular network formation [111]. Furthermore, as alginate does not have RGD molecules, which are responsible for cell attachment, synthetic peptides with RGD molecules are incorporated with alginate to improve cell growth [112].

2.2. Synthetic polymers

Synthetic polymers, such as poly(ethylene glycol) diacrylate (PEGDA), and poly(ethylene glycol)-tetra-acrylate (PEGTA), have been used for 3D bioprinting of vascularized constructs on account of their tailorable mechanical properties, processability and biocompatibility. PEGDA and PEGTA are PEG derived photocrosslinkable polymers which contain acrylate groups for photopolymerization. Therefore, PEGDA and PEGTA are commonly used for UV/visible light assisted printing techniques. The crosslinking rate of these two polymers ranges from several seconds to minutes depending on the type and concentration of photoinitiators [113]. The printability is affected by rheological properties which are dependant on molecular weight and concentration of polymers. As PEG itself is not an ideal material for cell growth due to the lack of cell-adhering moieties, PEGDA and PEGTA are normally combined with other cell-friendly materials such as GelMA to improve their cell response. PEGDA acts as a better scaffold for cell growth and spreading due to its branched tetravalent molecular structure and multiple active crosslinking sites which allow formation of more porous and stiffer structures [114,115].

Pluronic® is another frequently used synthetic polymer for 3D bioprinting of vascular networks. It is a polyoxyethylene–polyoxypropylene–polyoxyethylene (PEO–PPO–PEO) amphiphilic triblock copolymer which possesses thermoreversible gelation behaviour. Because of this characteristic, Pluronic® is usually used as a sacrificial biomaterial which can be removed leaving behind patterned vascular networks. By incorporating ECs and cell-friendly biomaterials such as GelMA, fibrin and collagen, vascular networks (5-500 μm) with angiogenic sprouting can be obtained [116–118]. However, the main disadvantage of using Pluronic® is the need for a low temperature ($< 4^{o}C$) to liquefy this polymer, which limits its application in other high-resolution printing techniques other than extrusion. Therefore, capillary-scale networks cannot be bioprinted by using Pluronic®.

3. Bioprinting techniques

3.1. Inkjet bioprinting

While inkjet printers have been ubiquitously used in offices and homes to print 2D texts and images on paper, researchers are more interested in exploring further potential functionalities of such printers to fabricate 3D biological constructs which require a precise deposition of biomaterials as droplets and high-resolution patterning on a specific substrate. Inkjet printing can work either with a single-ink system or a multiple-ink system, both approaches can precisely print single/multiple materials at micrometre resolution with essentially no restrictions on the geometric complexity of the spatial arrangement. Therefore, this technique has the potential to create constructs or cell scaffolds with complex internal structures, such as connected channels and pores, which are of great importance for cell growth. There are two main types of inkjet printing: (1) Continuous inkjet printing (CIJ) and (2) Drop-on-demand inkjet printing (DOD). However, CIJ has a few critical limitations, such as the risk of contamination of final products, the obligatory use of electrically conductive inks and low printing resolution. Therefore, DOD is the most common inkjet printing technique which has been extensively used for 3D bioprinting.

DOD inkjet printing generates droplets only at required places by propagating a pressure pulse in a fluid filled chamber. Because droplets are only ejected when required, the material waste is minimal compared to CIJ. DOD inkjet printing also minimises the risk of contamination of product because a recycling system is not needed, which means the ink used is always fresh. DOD inkjet printing can be further divided into two sub-types as shown in Fig. 1: (1) piezoelectric DOD inkjet printing, in which the formation of droplets occurs by mechanical actuation of a piezoelectric material which surrounds the ink chamber, this sudden volume change of the ink chamber generates droplets.

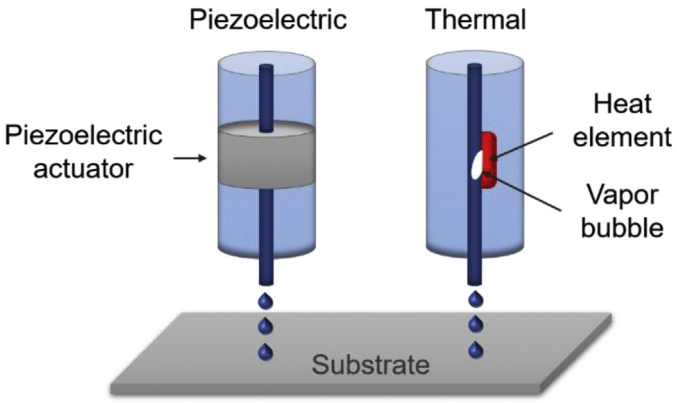

Fig. 1. Schematic illustrations of drop-on-demand (DOD) piezoelectric and thermal inkjet printing.

(2) Thermal DOD inkjet printing, in which a vapour bubble is generated by a heater/resistor which can vaporise a small volume of the ink causing a droplet to be ejected.

As mentioned earlier, different materials can be printed through individual channels using DOD inkjet printing, which allows for reactive inkjet printing, in which a droplet of one ink can be accurately printed on top of a deposited droplet of another ink, causing reactions and formation of product material at the specified positions [119]. Reactive inkjet printing is usually used to print materials which are insoluble or barely soluble to form printable liquid inks but can be formed through reaction with different liquid reactant materials. This approach opens a new window for printing materials and solidification mechanisms, thus facilitating formation of 3D constructs with tricky outer and inner structures.

Inkjet printing has been successfully used to print cell-laden materials with high post-printing cell viability which is the first step towards bioprinted 3D vascularized tissues [121,122]. As vascular networks have complex branches, one of the challenges is to print overhanging structures, especially without a supporting material. Improving the quality of overhanging structures and fully addressing this challenge is essential to the success of fabricating vascular networks. After the first successful tubular structure fabricated by inkjet printing in 2009 [123], Christensen et al. [120] reported that two vessel-like tubular structures with bifurcations were fabricated using reactive inkjet printing with alginate hydrogel. Fig. 2(a, b) schematically illustrates two setup configurations, in horizontal and vertical directions, for printing which can address the challenge of non-printability of overhanging structures. Fig. 2 (c-h) shows different views of inkjet-printed alginate tubular structures with or without cells. It was noticed that structures printed without cells had higher feature resolution than those printed with cells. This difference in resolution was due to the presence of cells in the bioink causing a poor quality of droplet formation and wider deposition trajectories during printing. The cell viability was tested to investigate the effect of the printing process on the living cells (NIH 3T3 mouse fibroblasts). It was found that the viability of the cell within the post-printed structure was 92.4% right after printing and 90.8% after 24 hours of incubation, indicating negligible effect of the printing process on the viability of the printed cells. However, the perfusion performance under long-term cell culture environment is missing in this early research. Another limitation is that this work did not integrate the bioprinted tubular structures with the parenchymal tissue for fabricating a functional vascularized tissue model as the 3D structures were printed directly into a crosslinker pool which did not have necessary constituents for cell culture and growth.

The main advantages of using inkjet printing as a 3D bioprinting strategy are: (1) using as low as pico-litre volume of materials which can dramatically save the costs of biomaterials, such as growth factors, hormones and enzymes, which are very expensive [124]; (2) precise control of deposition of droplets allowing a high, micrometre scale resolution [125]; (3) the non-contact characteristic of inkjet printing minimises the risk of cross-contamination of the final product, and the waste of material is minimised; (4) it is easy to introduce gradients in concentration or number of biomaterials or cells by altering the droplet size and frequency [126]. However, it also has intrinsic drawbacks: (1) limited choices of printable materials due to the specific requirements of viscosity and surface tension; (2) the mechanical stress and heat during jetting process may affect the activity of cells and sensitive biomaterials [124]; (3) the nozzle geometry may affect printing patterns at high resolution [125]; (4) clogging of the nozzle leading to irregular droplet sizes and directionality [124]; (5) difficulty in achieving large scale constructs due to the slow fabrication speeds of droplet-based printing; (6) cell aggregation and sedimentation in ink reservoir. However, inkjet printing offers the potential to fabricate multi-material and multi-scale constructs with complex vascular structures at a high printing resolution, as its building block, i.e. jetted droplet, has a very small volume in picolitre range [127].

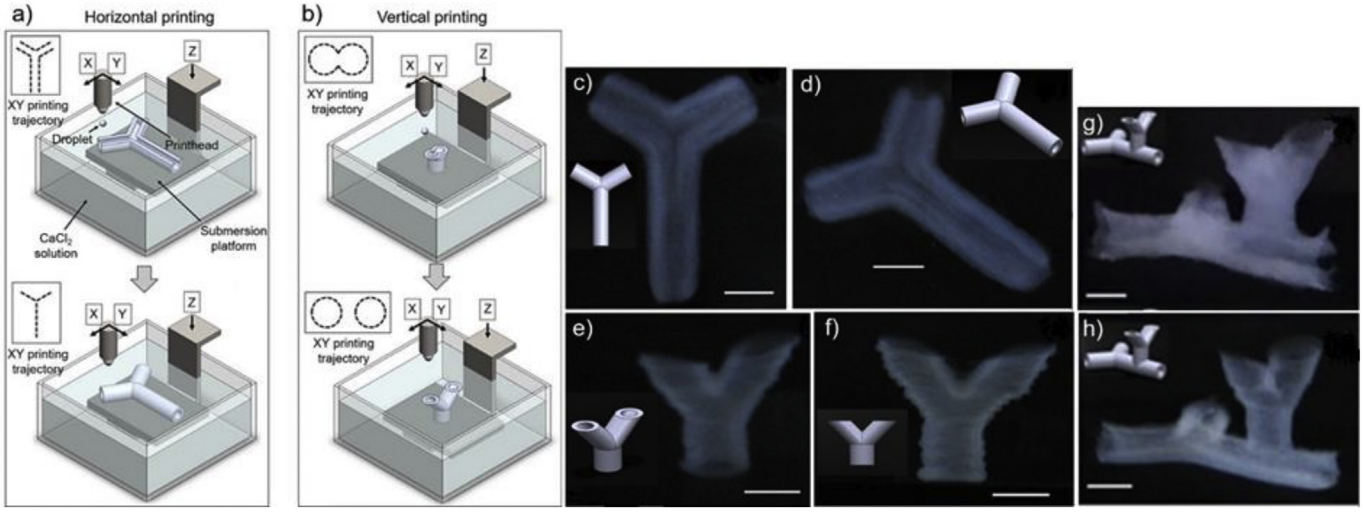

Fig. 2. (a, b) A schematic showing the inkjet printing system and the process with different printing directions. (c, d) Top and global view of a bifurcated structure using horizontal printing (without cells). (e, f) Top and global view of a bifurcated structure using vertical printing (without cells). (g, h) Global view of inkjet-printed structure with both horizontal and vertical bifurcations with (g) and without (h) cells. Scale bar, 3 mm. (images adapted from ref. [120] Copyright © 2014 Wiley-VCH)

3.2. Extrusion-based bioprinting

In the extrusion-based bioprinting, (bio)inks are dispensed by a deposition system which allows the precise deposition in the form of cylindrical filaments. The deposited (bio)inks require suitable solidification mechanisms to achieve good stability after printing. The key advantage of extrusion-based bioprinting is the high printing speed which allows large scalability in a short period of time. Additionally, extrusion-based bioprinting is also capable of printing cell-laden materials with high cell density which is essential for any potent post-biofabricated tissues/organs [128–131]. However, extrusion-based bioprinting also has its intrinsic drawbacks: (1) the resolution is normally low. Typically, the minimum size of final product is over 100 μm [132], resulting in the lack of precise patterning and organizing of cells; (2) the materials used in extrusion-based printing require the shear thinning ability to overcome their surface tension to ensure proper extrusion in the form of cylindrical filaments; (3) for cell-laden bioinks, the shear stress or the solidification methods may harm the viability of living cells.

3.2.1. Mechanical extrusion bioprinting

The bioinks used for mechanical extrusion-based bioprinting are formulated in semi-liquid or hydrogel form. The bioinks are then pushed out through a nozzle using either pneumatic pressure or a piston or a constantly forward-rotating screw inside the ink reservoir. Fig. 3(a) illustrates the pressure-driven and screw-driven extrusion printing. The piston-driven extrusion provides faster and better controllability over ink deposition in comparison to the pneumatic extrusion where the changes made in the gas volume takes longer time to show effect on the ink dispensing. Screw-driven extrusion are better suited for very high viscosity hydrogels. They are, however, less suitable for cell-laden hydrogels as the relatively higher pressure and shear stress may negatively affect the viability of the embedded cells. The rate of extrusion depends on the required geometric complexity and resolution of the construct being fabricated and on the physiochemical properties of the (bio)inks such as the solidification time and tolerance to shear stress. To maintain a self-standing structure, inks with higher viscosities than those used in droplet-based printing are used [133].

3.2.2. Thermal extrusion bioprinting

Fused deposition modelling (FDM) is a variant of extrusion-based printing. It is capable of fabricating 3D structures by depositing thermally softened materials, such as thermoplastics and sugars, through a heated nozzle as illustrated in Fig. 3(b). In FDM, solid state materials (e.g. filament, powder, pellet) are heated to a temperature near their specific melting point, and are then extruded out of a heated nozzle as semi-molten strings following predefined CAD based patterns to form layers. Once a layer is completed, the substrate/platform moves down in Z direction by a predefined distance (layer thickness) to start printing the next layer. Some commercial FDM machines can process multiple materials at a time, allowing more than one material to be deposited simultaneously, forming multi-material constructs, or using the second material as supporting or sacrificial material which can be easily removed after printing.

As aforementioned, a successfully engineered tissue/organ requires the fabrication of vascular networks with hierarchical and perfusable channels [134]. Currently, there are two approaches, which are direct and indirect printing, to achieve perfusable channels. Direct printing uses cell-laden or cell-compatible materials as (bio)inks which are required to possess relatively fast solidification rate to form a stable construct. However, direct printing of hollow channels has strict requirements in terms of materials, solidification mechanism, etc. which narrow down the choices of printable materials and printing methods. In order to address this challenge, the indirect printing approach prints sacrificial mold together with other supportive biomaterials to from a multi-material matrix system [135,136]. Once the printing process is finished, the sacrificial mold is removed to form the hollow structures. This method has been recently explored to better mimic native organ-specific tissues in terms of mechanical properties, geometries and biocompatibility [98,137–139].

Coaxial extrusion printing has been increasingly explored for direct 3D bioprinting of vascular constructs on account of their simplified printing process and scalability [140–144]. By precisely printing specific cell-laden bioinks according to the native blood vessel structure, the emulated vascular constructs can be achieved. Jia et al. [115] designed a multi-layered coaxial extrusion bioprinting system and successfully fabricated a range of cell-laden vascular constructs using a biocompatible hydrogel mixture containing GelMA, alginate and PEGTA. The solidification of the cell-laden hydrogel mixture was achieved by two-step crosslinking: ionical crosslinking of alginate and photo-crosslinking of GelMA and PEGTA as shown in Fig. 4(a). The printability of the mixture and the mechanical properties of the crosslinked construct can be tuned by altering the ratio between GelMA and PEGTA. The size of the vascularized constructs can be manipulated by using different designs of multi-layered coaxial nozzles (Fig. 4(b)). As can be seen from Fig. 4(c), vascularized constructs with different sizes were successfully fabricated. Moreover, the biocompatibility of the bioprinted vascularized constructs was validated as the embedded endothelial and stem cells

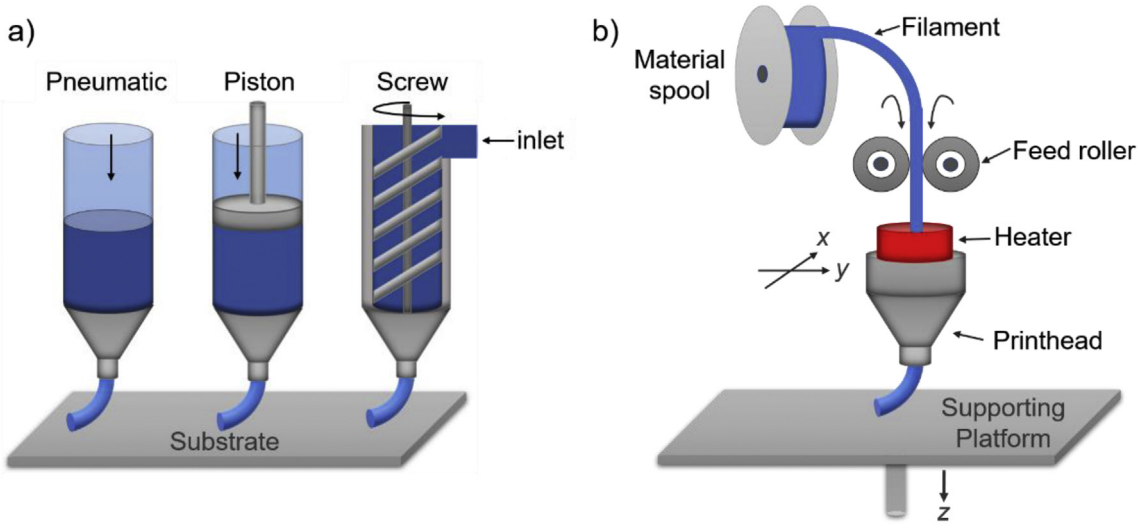

Fig. 3. Schematic illustrations of (a) mechanical extrusion, which has three main types according to the mode of operation; and (b) Fused deposition modelling (FDM).

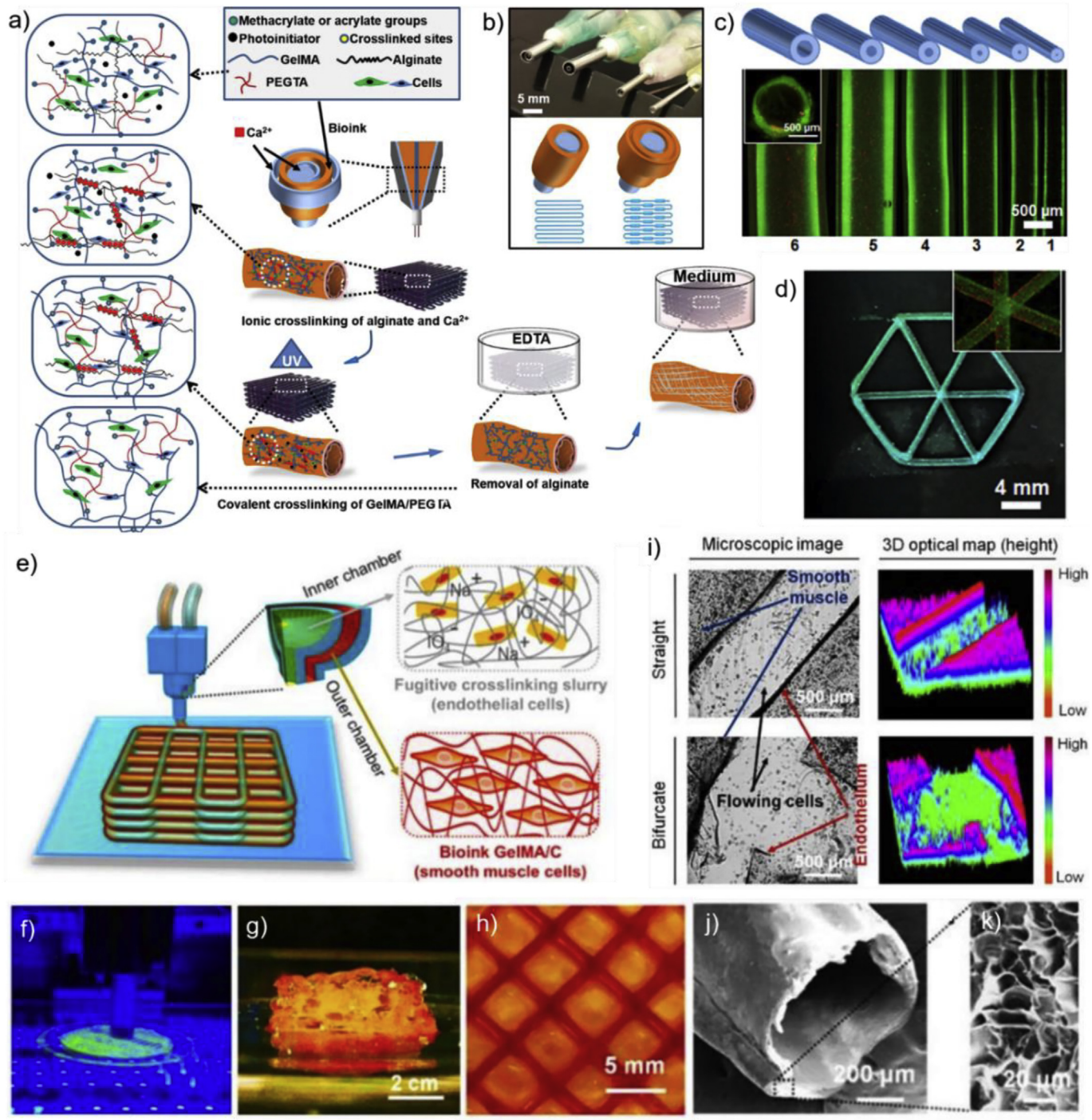

Fig. 4. Coaxial 3D extrusion bioprinting of vascular constructs. (a) A schematic showing the bioprinting process of the hollow channels which were achieved by two-step crosslinking of the cell-laden hydrogel mixture where alginate was crosslinked by $CaCl_2$; GelMA and PEGTA were crosslinked by UV. (b) The designed multi-layered coaxial nozzles and schematic diagram showing fabrication of perfusable hollow tubes with constant diameters and changeable sizes. (c) Fluorescence microscope images of the hollow channels fabricated by coaxial extrusion printing with different sizes. (d) Fluorescence microscope image of a perfusable vasculature which was illuminated by green fluorescent beads. The inset is the enlarged image of the perfusable hollow channels which were illuminated by red fluorescent beads. (images adapted from ref. [115] Copyright © 2016 Elsevier Ltd.) (e) A schematic showing the vascularized construct fabricated by coaxial 3D extrusion printing. (f) Photo image of the extrusion bioprinter. (g) The side view of the bioprinted vascular construct. (h) The top view of the vascular construct after 24h of perfusion culture. (i) Microscopic images and 3D optical maps of the bioprinted vasculature in straight and bifurcated regions. (j) SEM image of the cross-sectional morphology of bioprinted hollow channel. (k) Enlarged SEM image of the cross-sectional surface of the bioprinted hollow channel. (images adapted from ref. [145] Copyright © 2019 IOP Publishing Ltd.)

performed a good spreading and proliferation. Similarly, instead of printing the ECs together with the hydrogel to form the channel wall directly, Cui et al. [145] recently used the same method to fabricate self-standing and small-diameter vascularized constructs which is integrated with the SMCs and ECs to replicate the complexity and functionality of natural blood vessels. By coaxial printing of the inner (endothelial cell-loaded slurry) and outer (smooth muscle cell-loaded catechol-functionalised GelMA, GelMA/C) chambers followed by post crosslinking, the vascularized constructs with ECs were achieved without collapse as shown in Fig. 4(e-k). The authors claimed that the needle

(printhead) gauge can be easily replaced to fabricate vascularized constructs with different sizes to mimic the hierarchical vascular networks in native tissues. In order to increase the cell affinity, which results in improvement in generation of functional tissues, Gao et al. [146] used vascular-tissue-specific bioinks, i.e. combinations of vascular-tissue-derived extracellular matrix and alginate with ECs and vascular smooth muscle cells, respectively, to fabricate vascularized constructs by using coaxial extrusion printing. The advantage of this work over others was the *in vivo* study which showed excellent patency, well-retained endothelium, matured smooth muscles, and integration with host tissues. These pioneer works showed that the coaxial extrusion printing possesses the great promise of fabricating vascular constructs with high aspect ratio. The flexibility of dimensions, such as diameter and length, makes coaxial extrusion printing highly suitable for fabricating tubular constructs. However, using coaxial extrusion printing to print branched structures is yet to be achieved.

Although fabrication of vessel-like hollow channels has been successfully achieved as mentioned above, printing multi-scaled heterogeneous constructs is still required to match the native tissues. Most recently, Kang et al. [147] successfully fabricated a heterogeneous, multi-cellular, and multi-material construct which was aiming to mimic the liver unit, i.e. hepatic lobule, by using extrusion bioprinting of alginate and gelatin. Fig. 5(a) schematically shows the setup of the multi-scaled extrusion bioprinting. It can be seen that the fabricated hepatic lobule was composed of ECs, hepatocytes and lumen (hollow channel). By simultaneous printing of the three materials, a multi-scaled and vascularized biomimetic construct was obtained (Fig. 5 (b)). Fig. 5(c) shows the well-preserved structural integrity of the construct, fabricated by using the pre-set cartridge, after *in vitro* culture for 7 days, whereas the mix-printed sample showed inconsistencies in the structure. This is attributed to the spatial cell arrangement and enhanced cellular organization of each cell type.

However, the directly printed vascular constructs without supporting materials are prone to deform or collapse when printing tissues, especially organs with significantly larger dimensions and higher complexity. Therefore, an alternative 3D extrusion printing strategy has emerged which directly prints the large-sized constructs in a supporting medium. Noor et al. [98] used this method to successfully print a cellularized human heart with major blood vessels using cardiac and endothelial cell-laden hydrogels as shown in Fig. 6. The left and right ventricles of the printed heart were injected with red and blue dyes, respectively, in order to demonstrate hollow chambers and the septum in-between them as shown in Fig. 6(e). Similar method has been recently adopted to fabricate tumor models (glioma) to evaluate the mechanism of angiogenesis and tumor vascularization, which provides a feasible approach for fabricating microenvironment for vascularization [148].

Another method to address the issues associated with direct printing of vascularized constructs is indirect printing where a sacrificial mold is used. Recently, personalized thick and vascularized cardiac tissue has been fabricated using indirect 3D extrusion bioprinting. The bioink contained cardiomyocytes and ECs which were differentiated from

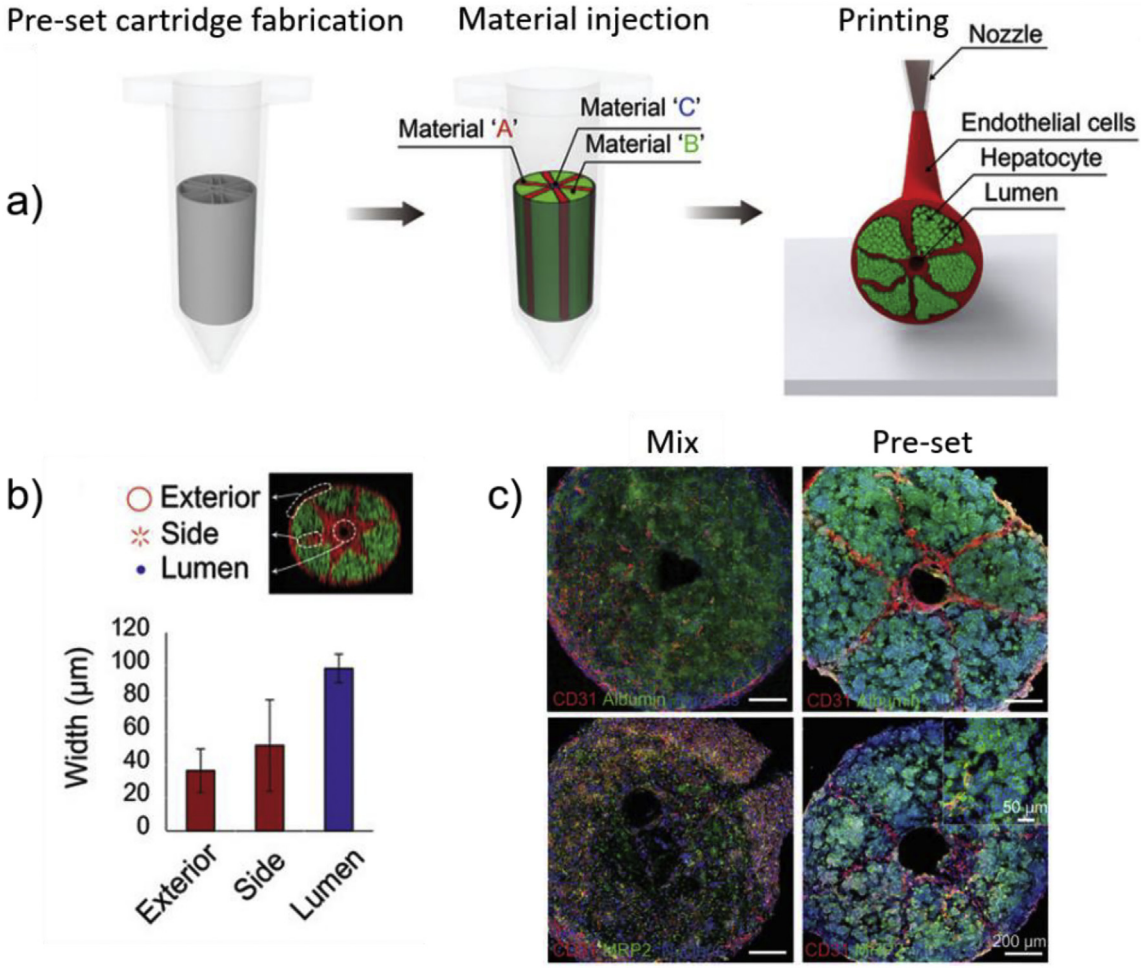

Fig. 5. (a) Schematic illustration of the pre-set extrusion bioprinting technique for hepatic lobule printing. (b) Average width of the printed construct. (c) Structural integrity inspection by immunostaining of CD31 (red), albumin (green), MRP2 (green), and nucleus with DAPI (blue) on day 7 post-printing. (images adapted from ref. [147] Copyright © 2020 Wiley-VCH).

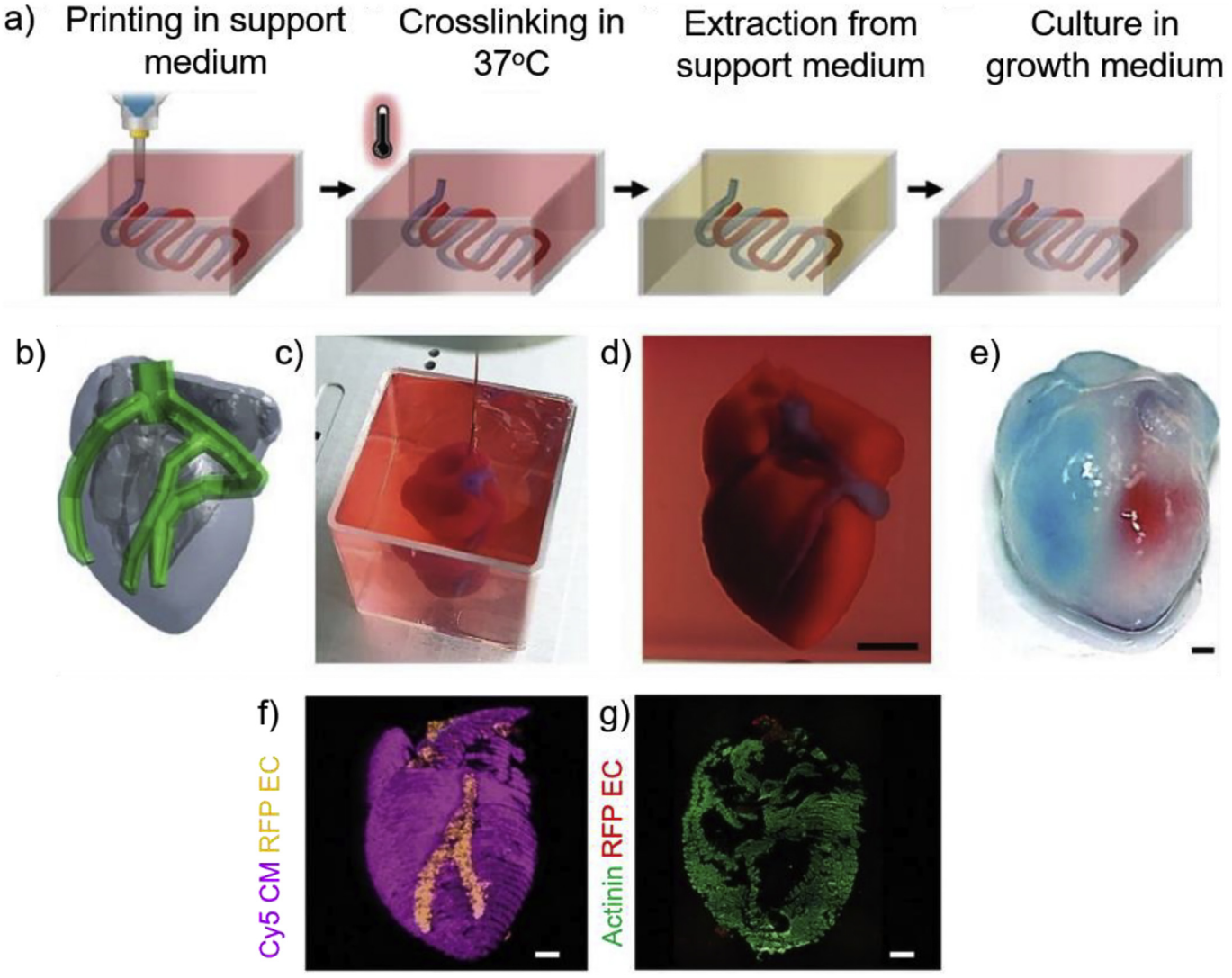

Fig. 6. (a) Schematic illustration of 3D constructs fabricated in a supporting medium using mechanical extrusion printing. (b) The human heart CAD model. (c, d) A printed heart within a supporting material bath. (e) A printed heart with major blood vessels after crosslinking. Blue and red dyes demonstrate the hollow chambers created in the heart. (f) 3D confocal image of the printed heart (cardoimyocytes (CMs) in pink, endothelial cells (ECs) in orange). Scale bar, 1 mm. (g) Cross-sections of the heart immunostained against sarcomeric actinin (in green). Scale bar, 1 mm. (images adapted from ref. [98] Copyright © 2019 American Association for the Advancement of Science)

patient's reprogrammed hiPSCs. Therefore, the final printed constructs fully match the immunological, biochemical and anatomical properties of the patient [98]. Skylar-Scott et al. [139] also used hiPSCs and indirect 3D extrusion printing to successfully fabricate a vascularized cardiac tissue. As sacrificial material was used to create hollow vascular channels which were embedded in the matrix, the authors named this biomanufacturing method as sacrificial writing into functional tissue (SWIFT) as shown in Fig. 7(a). In order to investigate the effect of the vascular networks on the cell viability after printing, a perfusable tissue with high cell density and vascular channels was fabricated as shown in Fig. 7(b, left). After removing the sacrificial ink, gelatine, the vascular channels were perfused with hyperoxygenated medium (95% O_2, 5% CO_2) at a flow rate of 250 μL/min for 12 hours. It can be seen from Fig.7(b, right) that the printed vascular channels remained as hollow channels and cells remained viable. To demonstrate the ability of fabrication of organ-specific tissue by using SWIFT, a cardiac structure with an arterial vascular network geometry was fabricated as shown in Fig. 7(c). The most advantageous development of this work over other embedded printing for organ-specific tissue fabrication is the long-term perfusion test and the prolonged cell viability *in vitro*. This work paves the way towards the fabrication of personalised organ-specific tissues with high cell density and vascular networks for therapeutic applications.

Using thermal extrusion bioprinting to fabricate vascularized constructs was firstly introduced by Miller et al. [149] using an FDM printer in 2012. The concept was to print a sacrificial mold (carbohydrate glass) which was subsequently cast with cell-laden hydrogels such as alginate, PEG, agarose and Matrigel. After casting, the sacrificial mold was removed from the cell-laden hydrogels to create perfusable channels as shown in Fig. 8(a, b). The author claimed that the channel networks can be perfused within minutes and support the lining of the ECs (Fig. 8(c)). However, it is difficult to create complex sacrificial molds without printing support materials. In order to create complex vascular networks, Pimentel C. et al. [150] employed Poly(lactic acid) (PLA) as the support material to generate Poly(vinyl alcohol) (PVA) sacrificial molds using FDM, as shown in Fig. 8(d). After printing, the Poly(lactic acid) (PLA) was removed leaving behind the water-soluble PVA sacrificial mold (Fig. 8(e-g)). Like Miller's work, the sacrificial mold was subsequently cast with a cell-laden ECM followed by a thorough perfusion to remove the sacrificial PVA mold. However, there was difficulty in creating hollow channels with diameter less than 1 mm due to the

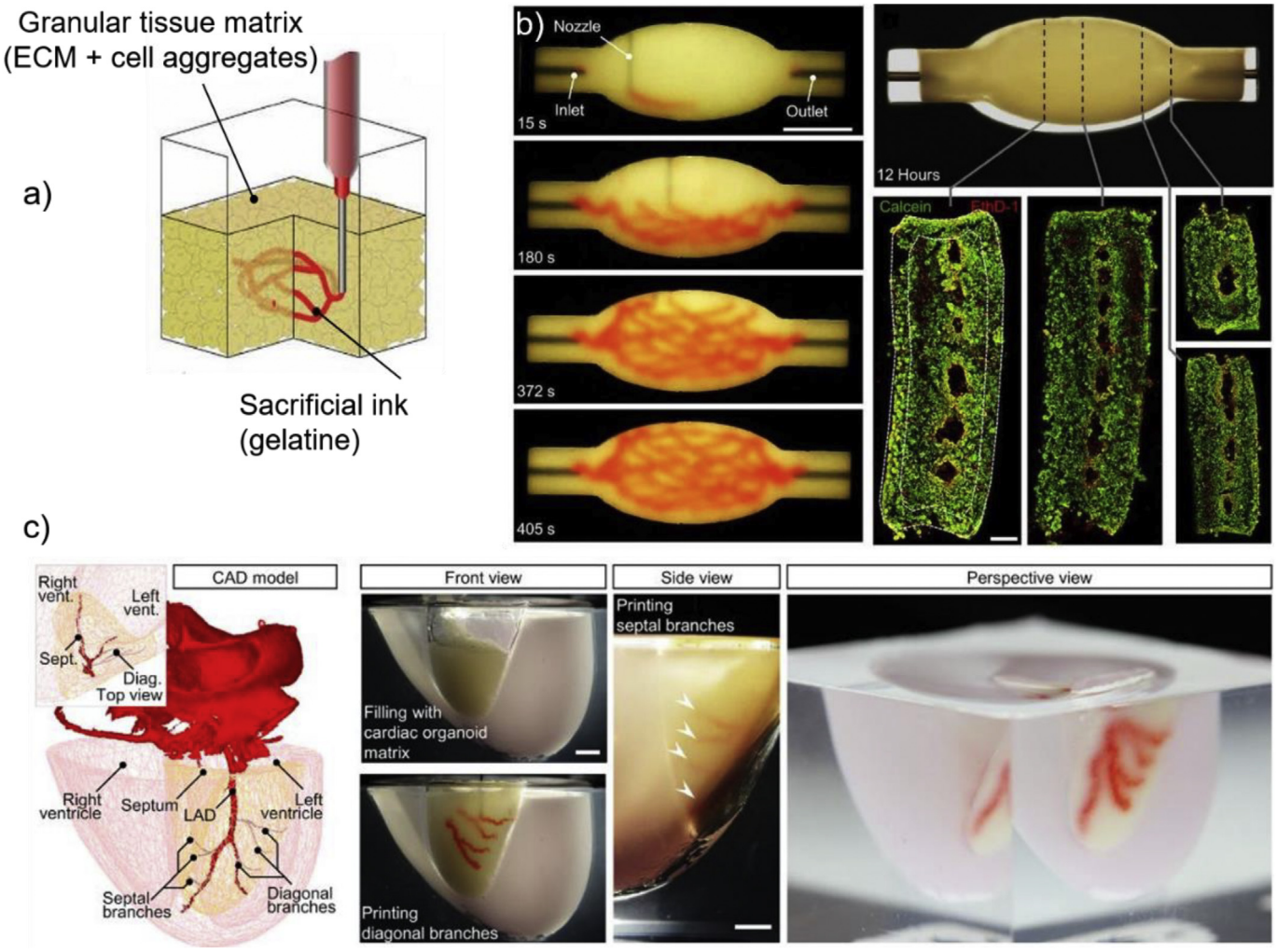

Fig. 7. Sacrificial writing into functional tissue. (a) A schematic illustration of the printing step. (b) Sequential images showing the fabrication of a perfusable tissue with vascular channels by extrusion-based printing within the tissue matrix connected to inlet and outlet tubes. Scale bar, 10 mm. (c) 3D model of a normal human heart used as a template for the printing (left); different view of a 1:2 scale polydimethylsiloxane cardiac tissue with septal branches fabricated by extrusion-based printing. Scale bar, 5 mm (right). (images adapted from ref. [139] Copyright © 2019 American Association for the Advancement of Science)

weakness of PVA, indicating that a stronger sacrificial material is needed if creating minute capillary networks. Additionally, the fabricated vasculature cast in a soft hydrogel could maintain its structural integrity after two weeks' perfusion, which facilitated the long-standing *in vitro* biological tests. Excellent cell viability was also achieved, which was attributed to the good perfusability of the vascularized construct.

While extrusion-based bioprinting is capable of fabricating complex vascular networks in the relatively large sized constructs through direct or indirect printing, 3D vascular networks with hierarchical sized vessels have not been reported yet. Furthermore, using current extrusion-based bioprinting technique to fabricate micrometre-scale capillaries is not feasible due to its inherent low printing resolution.

3.3. Stereolithography (SLA)

In stereolithography (SLA), photochemically reactive inks, which can be cross-linked with infra-red, UV and high-intensity laser, are used for fabrication of 3D structures with micron-scale resolution. In SLA, light acts as an etching agent to remove inks from certain locations for obtaining the desired structure on the substrates. Fig. 9(a) schematically shows the conventional SLA which is capable of developing tissue scaffolds with more than one spatially distributed microenvironments and helps in lineage differentiation when stem cells are cultured on them with different growth factors in different microenvironments [151]. This is an important step in the direction towards full-scale *in vitro* organ printing and maturation.

Continuous liquid interface production (CLIP) is an upside-down form of SLA, in which, the curing light is used to illuminate the resin bath from below through a transparent window at the base of the resin bath container as shown in Fig. 9(b). The support plate on which the structure is fabricated is dipped into the resin bath from top. As curing light is shown according to the 3D CAD model, the resin forms structure on the support plate, which is continuously moved upwards allowing fresh resin to fill the gap and the structure to grow in size [152].

SLA has been successfully used to create vascular networks for circulation of oxygen and cell growth gradients [153,155]. Cui et al. [153] recently employed SLA to fabricate a 3D vascularized model to investigate the breast cancer metastasis to bone. By using a light crosslinkable material, GelMA/PEGDA with or without nano-hydroxyapatite (nHA), the author successfully printed a 3D vascularized construct which consists of three chambers: micro-vascularized bone, endothelialized vessel and cancer tumour as shown in Fig. 10(a-d). This 3D printed cancer model provides an approach to mimic transendothelial migration and colonization of cancer cells, which paves the way towards the screening of novel anticancer drugs and the development of customised

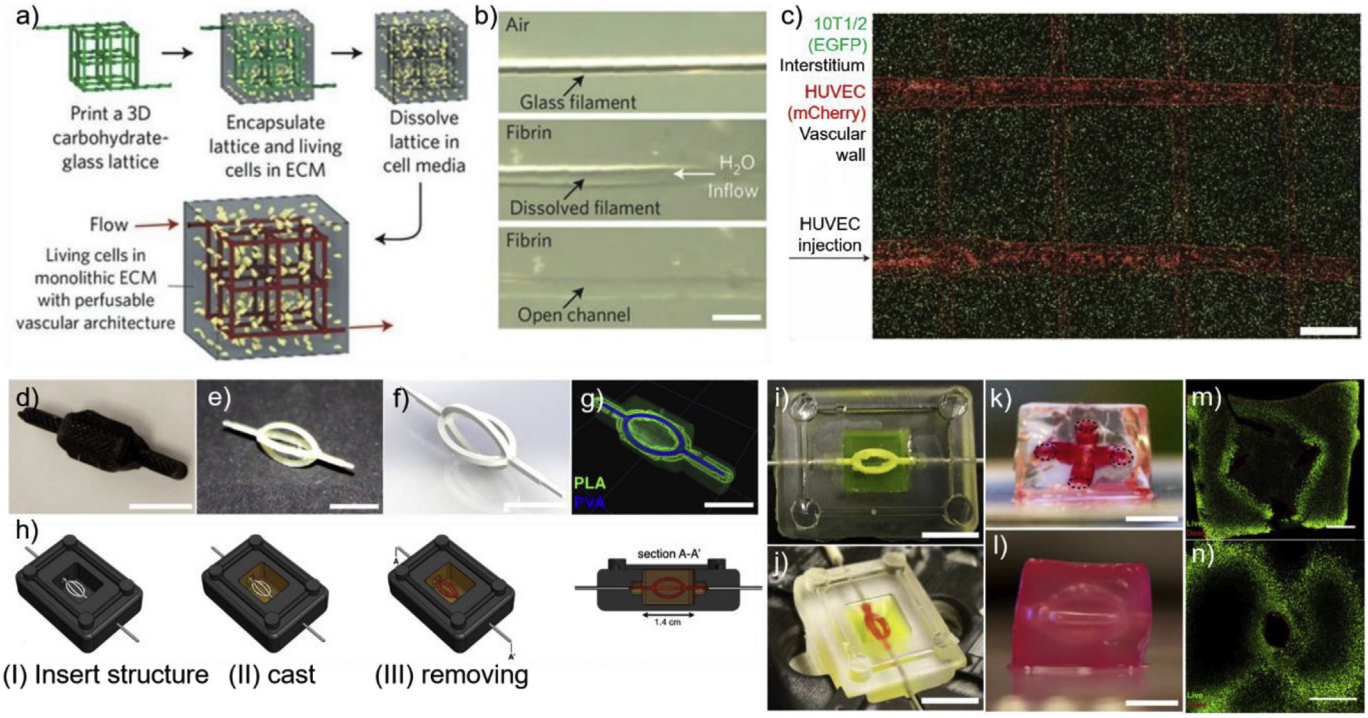

Fig. 8. Vascular networks fabricated by thermal extrusion bioprinting (FDM). (a) A schematic illustration of the vascularized construct fabricated by FDM. (b) A single carbohydrate-glass fibre (200 μm in diameter, top) is encapsulated in a fibrin gel. After removing the carbohydrate-glass, an open perfusable channel in the fibrin gel was created. Scale bar, 500 μm. (c) A confocal image of the vascular network embedded with 10T1/2 cells and seeded with endothelial cells after 24 h culture. Scale bar, 1 mm. (images adapted from ref. [149] Copyright © 2012 Macmillan Publishers Limited) (d) A photograph of the FDM printed mold with four curved arms using PVA as sacrificial material and PLA as support material. (e) A photograph of the PVA mold after removing the PLA support material. Scale bar, 3 mm. (f) A CAD model of the designed sacrificial mold. (g) The visualized motion program of the sacrificial mold. Scale bars, 6 mm. (h) A schematic show of the fabrication processes of the vascular construct. (i) A photograph of the sacrificial mold cast in a gelatin hydrogel before removing PVA. (j) A photograph of the vascularized construct after removing PVA. Scale bars, 1.4 cm. (k) A photograph of the cross-section of the vascularized construct, showing the volumetric distribution and structural stability of the channels. Scale bar, 5 mm. (l) A photograph of vascularized construct after 24 h of direct perfusion. Scale bar, 4.5 mm. (m, n) Live/dead confocal microscopy images of the cross-section in the centre with the four channels (m) and the inlet of the perfusion (n) of a 1 cm thick vascularized construct after 15 days of cell culture. Scale bar, 2 mm. (images adapted from ref. [150] Copyright © 2017 Acta Materialia Inc.)

diagnostics and therapeutics. In order to fabricate complex 3D vascular networks which better mimic the native tissue, Grigoryan et al. [154] used SLA to create a range of intravascular and multi-vascular networks within biocompatible hydrogels as shown in Fig. 10(e-h). After successfully creating the entangled perfusable networks in PEGDA hydrogel (Fig. 10(e)), the authors extended the work to create a lung mimetic unit which comprised an inlet and outlet vascularized network and air sac as shown in Fig. 10(f). The perfusion test demonstrated that the printed vascularized hydrogel (PEGDA) could withstand more than 10,000 ventilation cycles over 6 hours during red blood cells (RBC) perfusion while switching the inflow gas between humidified oxygen and humidified nitrogen. With the goal of fabricating structurally complex and functional tissues, a multi-material liver tissue was created by seeding the vascularized hydrogel carriers containing hepatocyte aggregates with ECs as shown in Fig. 10(g, h). The *in vivo* biocompatibility test demonstrated the surviving functional hepatocytes, confirming the biocompatibility of the printed vascularized tissue. This work made the preclinical studies possible by providing an approach to overcome the long-standing design hurdle in functional tissue fabrication.

The main advantage of both SLA and CLIP is that they offer highly scalable 3D bioprinting similar to extrusion-based printing, while not compromising with the high resolution similar to inkjet printing. The

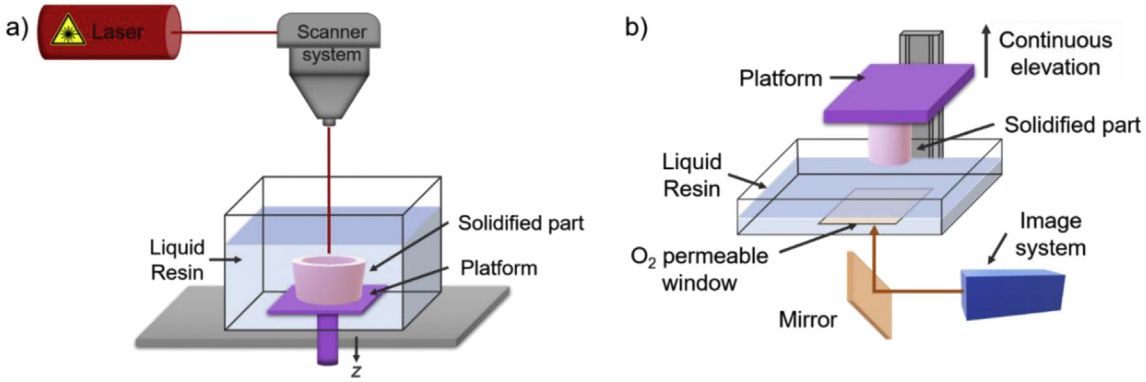

Fig. 9. Schematic illustrations of (a) conventional stereolithography; and (b) Continuous liquid interface production (CLIP).

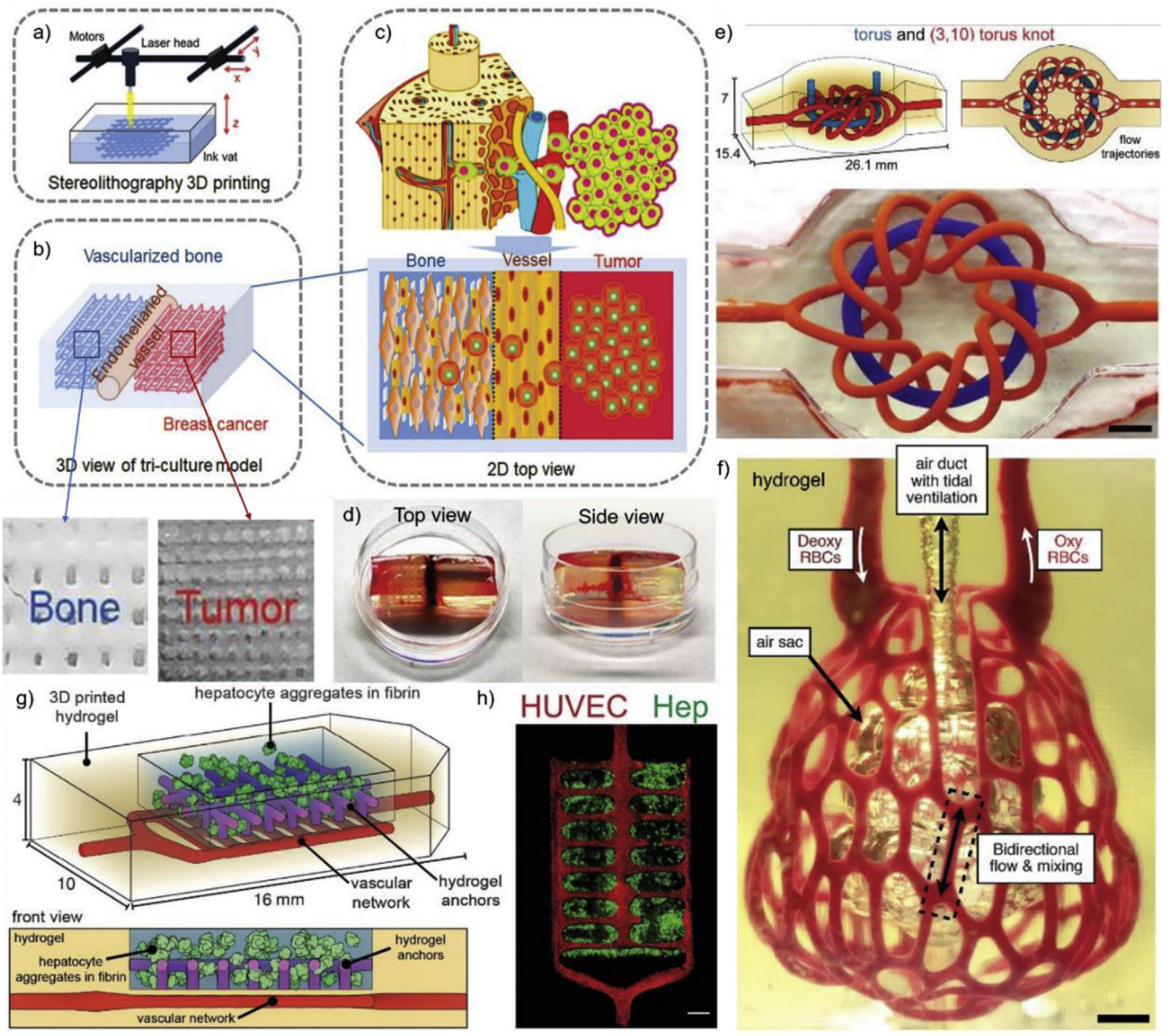

Fig. 10. Vascularized constructs fabricated by SLA. (a) Beam-scanning SLA printing of breast cancer bone model. (b) A schematic 3D view of the triculture model. (c) A schematic of the *in vivo* invasion of cancer cells into bone and 2D view of the triculture model. (d) Photo images of 3D printed breast cancer model with top view and side view (the thickness of the model construct is ≈3 mm). (images adapted from ref. [153] Copyright © 2019 Wiley-VCH) (e) Top: A schematic illustration of a designed entangled vessel topology. Bottom: A photograph of the SLA printed vessels in hydrogel (20 wt% PEGDA). Scale bar, 3 mm. (f) A photograph of the SLA printed vasculature during perfusion while the air sac was ventilated with oxygen. Scale bar, 1mm. (g) Vascularized hepatic hydrogel carriers were created by seeding HUVECs in the vascular network after printing. (h) Confocal microscopy observations show that hydrogel anchors physically entrap fibrin gel containing the hepatocyte aggregates. Scale bar, 1 mm. (images adapted from ref. [154] Copyright © 2019 American Association for the Advancement of Science)

main limitation is that they can be used only with photo-curable inks which normally are not biocompatible and biodegradable.

3.4. Laser-assisted bioprinting

Laser-assisted bioprinting was initially developed for printing of metals and electronic components. This technology has now been imported for printing living cells directly from cell culture suspensions at a specific location with a low margin of error of ± 5 μm in resolution on 2D or 3D substrates [156]. Based on different laser sources and energy absorbing layers, there are a few variations of laser-assisted bioprinting including laser guided direct write (LGDW), laser induced forward transfer (LIFT), absorbing film-assisted laser induced forward transfer (AFA-LIFT), matrix-assisted pulsed laser evaporation direct write (MAPLE-DW) and biological laser printing (BioLP). LGDW differs from the others as it uses weakly focused continuous laser while the rest four use pulsed laser. The main difference with LIFT is the use of high-powered pulsed laser and a thin absorbing layer between the donor slide and the bioinks. AFA-LIFT and BioLP use a thick absorbing layer that prevents the direct interaction between laser and the bioinks. MAPLE-DW uses a low-powered pulsed laser at UV or near-UV wavelength. Fig. 11(a) schematically shows a representative laser-assisted bioprinting: a pulsed laser beam is guided through mirrors onto a liquid film/bioink which is supported on a thin and transparent solid surface, e.g. quartz. The liquid film/bioink is a suspension of the cells that are to be deposited on the substrate. The amount of energy required to

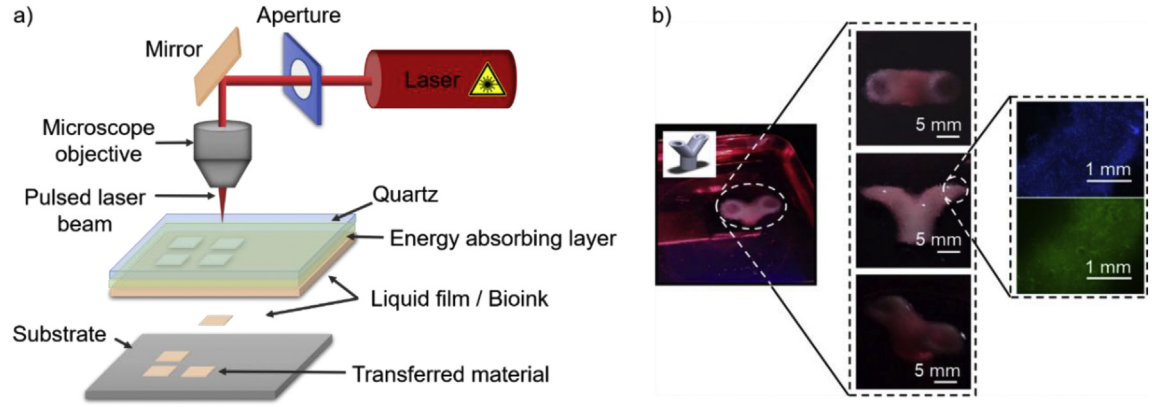

Fig. 11. (a) A schematic illustration of laser-assisted bioprinting process. (b) Images of the Y-shaped hollow channels fabricated by laser-assisted bioprinting using cell-laden hydrogel. (images adapted from ref. [159] Copyright © 2015 IOP Publishing Ltd.)

generate the laser pulses depends on the laser wavelength, beam thickness and the characteristics and thickness of the liquid film. When the laser is fired, its energy is absorbed by the liquid film leading to the formation of a tiny vapour bubble. The sudden expansion of the vapour bubble causes a tiny volume of the liquid to leave the film surface and fall on the receiver substrate to form transferred material. The volume of the deposited liquid depends on the laser energy and the liquid. The laser is guided and fired according to a pre-determined pattern leading to patterned cell-laden material on the receiver substrate [157]. Cell viability after laser-assisted bioprinting is affected by three main parameters, i.e. laser pulse energy, liquid film thickness and viscosity. Catros et al. [158] investigated a range of these three parameters found that the cell viability was enhanced by increasing bioink viscosity and film thickness, whilst increasing the laser energy has a negative effect on the viability of the printed cells.

Although laser-assisted bioprinting offers high printing resolution and is free from nozzle clogging, it is generally limited to fabricate 2D patterns due to its intrinsic printing mechanism. Photonic cell damage, cytotoxicity induced by using metal energy absorbing layer in LIFT and AFA-LIFT and limited scalability are the main disadvantages of using this method [21,160]. However, there is increased interest in using laser-assisted bioprinting to fabricate 3D vascular constructs/hollow channels for biomedical applications on account of its nozzle-free characteristic and precise deposition of materials [159,161]. Moreover, it can use biomaterials with high viscosities as printing inks which cannot be used by other techniques mentioned above. Xiong et al. [159] successfully fabricated straight and Y-shaped hollow channels using cell-laden alginate by laser-assisted bioprinting as shown in Fig. 11(b). No support structure was required for the printing of the branched Y-shaped tube, demonstrating the feasibility of this technique when applied to fabricate overhanging structures. The cell viabilities of the Y-shaped constructs immediately after printing and after 24 h incubation were 68.1% and 70.8%, respectively, with both being higher than that of the straight ones. This was attributed to the low landing force for printing overhang structures, hence resulting in a relatively higher cell viability.

4. Challenges and future prospects

In vitro vascularization in a tissue-engineered construct is of great importance for the supply of oxygen and nutrients and excretion of wastes after implantation *in vivo*. Especially for tissues with high level of oxygen consumption rate, suitable vascularization is essential to the final success of the implantation. Although current 3D bioprinting technologies have made a remarkable breakthrough in fabrication of vascular networks, there is still a big gap between perfusable tubular structures and vasculature. As blood vessels have layered structures with specific cells and proteins, the first challenge is to biologically mimic the layered structures of vessels to enable proper functions. Another vital challenge of 3D bioprinting of vascularized tissues lies in the accurate production of the complex hierarchical vascular networks which match the host tissues and the precise positioning of biomaterials, ECs, vascular SMCs and growth factors to improve vasculature. Current techniques have limitations in printing vessels from micrometre-scale to millimetre-scale in a single printing process. Furthermore, printing micrometre-scale functional capillaries, which have the equivalent importance to larger sized vessels for functional vascularized tissues, is yet to be achieved. One promising approach is to formulate bioinks with vascularization bioactives which can facilitate angiogenesis to form capillaries. This will require a good understanding of embryonic development, mechanobiology, cell-cell/cell-material interactions and biological responses of ECs to stimuli, such as perfusate flow and hydrostatic pressure. Biomaterials also need to be further formulated to be more supportive for cell growth with suitable mechanical properties, while maintaining good tissue structures without collapse in perfusion environment. Another aspect to be improved is the compatibility of biomaterials with current printing techniques in terms of printability, which determines the shape fidelity of printed structures.

Technologically, further efforts will be made to print a wider range of materials including matrix materials, cells and growth factors in accurate positions simultaneously with high resolution and printing speed. Multi-nozzle systems of various sizes, integrated into a bioprinter and independently dispensing multiple biomaterials, may be a promising approach to print highly scalable multi-material constructs at a high speed. Additionally, integration of different printing techniques can be a promising avenue to overcome current technical bottlenecks of 3D bioprinting. For instance, extrusion-based bioprinting, which suffers from low resolution while possessing high printing speed, can be combined with high resolution printing techniques, such as inkjet printing or laser-assisted printing, to fabricate large volumetric tissues with multi-scaled vascular networks.

In addition to fabricating vascularized tissues *in vitro*, direct printing of tissue-engineered constructs *in vivo* would be highly expected as the transplantation associated issues would be eliminated. By incorporating patients' anatomical clinical images, highly customized tissue constructs can be precisely printed *in vivo* during surgery, which will drastically reduce the treatment procedures of the conventional transplantation strategy.

Furthermore, 4D bioprinting has attracted increasing attention, and is believed to be the next generation of biofabrication technique. As 4D bioprinting is capable of fabricating dynamic 3D biological constructs that can be stimulated to change behaviours by using stimuli-responsive materials [162], therefore, the smart bioinks including ECs, growth factors can be dynamically controlled to biomimic the natural vasculature development via 4D printing.

Declaration of Competing Interest

The authors declare no conflict of interest.

Acknowledgements

The authors would like to thank the EPSRC (EP/N007174/1 and EP/N023579/1), Royal Society (RG160662) and Jiangsu specially appointed professor program for support.

References

[1] C.W. Hull, Apparatus for Production of Three-Dimensional Objects by Stereolithography, United States Patent, Appl., No. 638905, Filed 1984.
[2] S.C. Joshi, A.A. Sheikh, 3D printing in aerospace and its long-term sustainability, Virtual Phys. Prototyp. 10 (4) (2015) 175–185.
[3] P. Rokicki, B. Kozik, G. Budzik, T. Dziubek, J. Bernaczek, L. Przeszlowski, O. Markowska, B. Sobolewski, A. Rzucidlo, Manufacturing of aircraft engine transmission gear with SLS (DMLS) method, Aircraft Eng. Aerospace Technol.: Intern. J. 88 (3) (2016) 397–403.
[4] J.H. Martin, B.D. Yahata, J.M. Hundley, J.A. Mayer, T.A. Schaedler, T.M. Pollock, 3D printing of high-strength aluminium alloys, Nature 549 (7672) (2017) 365.
[5] M. Savastano, C. Amendola, D. Fabrizio, E. Massaroni, 3-D Printing in the Spare Parts Supply Chain: An Explorative Study in the Automotive Industry, Digitally Supported Innovation, Springer, 2016 153–170.
[6] S.R. Shin, R. Farzad, A. Tamayol, V. Manoharan, P. Mostafalu, Y.S. Zhang, M. Akbari, S.M. Jung, D. Kim, M. Comotto, A bioactive carbon nanotube-based ink for printing 2D and 3D flexible electronics, Adv. Mater. 28 (17) (2016) 3280–3289.
[7] A.D. Valentine, T.A. Busbee, J.W. Boley, J.R. Raney, A. Chortos, A. Kotikian, J.D. Berrigan, M.F. Durstock, J.A. Lewis, Hybrid 3D printing of soft electronics, Adv. Mater. 29 (40) (2017) 1703817.
[8] L.Y. Zhou, J.Z. Fu, Q. Gao, P. Zhao, Y. He, All-printed flexible and stretchable electronics with pressing or freezing activatable liquid-metal-silicone inks, Adv. Funct. Mater. 30 (3) (2020) 1906683.
[9] Y. Zhang, C. Tse, D. Rouholamin, P. Smith, Scaffolds for tissue engineering produced by inkjet printing, Central Eur. J. Eng. 2 (3) (2012) 325–335.
[10] C.M.B. Ho, A. Mishra, P.T.P. Lin, S.H. Ng, W.Y. Yeong, Y.J. Kim, Y.J. Yoon, 3D printed polycaprolactone carbon nanotube composite scaffolds for cardiac tissue engineering, Macromol. Biosci. 17 (4) (2017) 1600250.
[11] X. Yang, Z. Lu, H. Wu, W. Li, L. Zheng, J. Zhao, Collagen-alginate as bioink for three-dimensional (3D) cell printing based cartilage tissue engineering, Mater. Sci. Eng. C 83 (2018) 195–201.
[12] A. De Mori, M. Peña Fernández, G. Blunn, G. Tozzi, M. Roldo, 3D printing and electrospinning of composite hydrogels for cartilage and bone tissue engineering, Polymers 10 (3) (2018) 285.
[13] S. You, J. Li, W. Zhu, C. Yu, D. Mei, S. Chen, Nanoscale 3D printing of hydrogels for cellular tissue engineering, J. Mater. Chem. B 6 (15) (2018) 2187–2197.
[14] X. Du, D. Wei, L. Huang, M. Zhu, Y. Zhang, Y. Zhu, 3D printing of mesoporous bioactive glass/silk fibroin composite scaffolds for bone tissue engineering, Mater. Sci. Eng. C 103 (2019) 109731.
[15] Z. Wang, R. Abdulla, B. Parker, R. Samanipour, S. Ghosh, K. Kim, A simple and high-resolution stereolithography-based 3D bioprinting system using visible light crosslinkable bioinks, Biofabrication 7 (4) (2015), 045009.
[16] X. Liu, S. Michael, K. Bharti, M. Ferrer, M.J. Song, A biofabricated vascularized skin model of atopic dermatitis for preclinical studies, Biofabrication 12 (3) (2020), 035002.
[17] Y. Song, X. Su, K.F. Firouzian, Y. Fang, T. Zhang, W. Sun, Engineering of brain-like tissue constructs via 3D Cell-printing technology, Biofabrication 12 (3) (2020), 035016.
[18] G. Brunello, S. Sivolella, R. Meneghello, L. Ferroni, C. Gardin, A. Piattelli, B. Zavan, E. Bressan, Powder-based 3D printing for bone tissue engineering, Biotechnol. Adv. 34 (5) (2016) 740–753.
[19] R. Lozano, L. Stevens, B.C. Thompson, K.J. Gilmore, R. Gorkin, E.M. Stewart, M.I.H. Panhuis, M. Romero-Ortega, G.G. Wallace, 3D printing of layered brain-like structures using peptide modified gellan gum substrates, Biomaterials 67 (2015) 264–273.
[20] A.K. Gaharwar, A. Arpanaei, T.L. Andresen, A. Dolatshahi-Pirouz, 3D biomaterial microarrays for regenerative medicine: current state-of-the-art, emerging directions and future trends, Adv. Mater. 28 (4) (2016) 771–781.
[21] S. Vijayavenkataraman, W.C. Yan, W.F. Lu, C.H. Wang, J.Y.H. Fuh, 3D bioprinting of tissues and organs for regenerative medicine, Adv. Drug Deliv. Rev. 132 (2018) 296–332.
[22] J.I. Lipton, M. Cutler, F. Nigl, D. Cohen, H. Lipson, Additive manufacturing for the food industry, Trends Food Sci. Technol. 43 (1) (2015) 114–123.
[23] F.C. Godoi, S. Prakash, B.R. Bhandari, 3d printing technologies applied for food design: status and prospects, J. Food Eng. 179 (2016) 44–54.
[24] Z. Liu, M. Zhang, B. Bhandari, Y. Wang, 3D printing: printing precision and application in food sector, Trends Food Sci. Technol. 69 (2017) 83–94.
[25] J. Goole, K. Amighi, 3D printing in pharmaceutics: a new tool for designing customized drug delivery systems, Int. J. Pharm. 499 (1-2) (2016) 376–394.
[26] A. Goyanes, U. Det-Amornrat, J. Wang, A.W. Basit, S. Gaisford, 3D scanning and 3D printing as innovative technologies for fabricating personalized topical drug delivery systems, J. Control. Release 234 (2016) 41–48.
[27] A. Maroni, A. Melocchi, F. Parietti, A. Foppoli, L. Zema, A. Gazzaniga, 3D printed multi-compartment capsular devices for two-pulse oral drug delivery, J. Control. Release 268 (2017) 10–18.
[28] L.K. Prasad, H. Smyth, 3D Printing technologies for drug delivery: a review, Drug Dev. Ind. Pharm. 42 (7) (2016) 1019–1031.
[29] W. Zhu, B. Holmes, R.I. Glazer, L.G. Zhang, 3D printed nanocomposite matrix for the study of breast cancer bone metastasis, Nanomedicine 12 (1) (2016) 69–79.
[30] J.C. Lindegaard, M.L. Madsen, A. Traberg, B. Meisner, S.K. Nielsen, K. Tanderup, H. Spejlborg, L.U. Fokdal, O. Nørrevang, Individualised 3D printed vaginal template for MRI guided brachytherapy in locally advanced cervical cancer, Radiother. Oncol. 118 (1) (2016) 173–175.
[31] S. Knowlton, S. Onal, C.H. Yu, J.J. Zhao, S. Tasoglu, Bioprinting for cancer research, Trends Biotechnol. 33 (9) (2015) 504–513.
[32] Y. Li, T. Zhang, Y. Pang, L. Li, Z.-N. Chen, W. Sun, 3D bioprinting of hepatoma cells and application with microfluidics for pharmacodynamic test of Metuzumab, Biofabrication 11 (3) (2019), 034102.
[33] S. Swaminathan, Q. Hamid, W. Sun, A.M. Clyne, Bioprinting of 3D breast epithelial spheroids for human cancer models, Biofabrication 11 (2) (2019), 025003.
[34] H. Tseng, J.A. Gage, W.L. Haisler, S.K. Neeley, T. Shen, C. Hebel, H.G. Barthlow, M. Wagoner, G.R. Souza, A high-throughput in vitro ring assay for vasoactivity using magnetic 3D bioprinting, Sci. Rep. 6 (2016) 30640.
[35] Y.R. Liang, L.N. Zhu, J. Gao, H.X. Zhao, Y. Zhu, S. Ye, Q. Fang, 3D-printed high-density droplet array chip for miniaturized protein crystallization screening under vapor diffusion mode, ACS Appl. Mater. Interfaces 9 (13) (2017) 11837–11845.
[36] E.A. Roth, T. Xu, M. Das, C. Gregory, J.J. Hickman, T. Boland, Inkjet printing for high-throughput cell patterning, Biomaterials 25 (17) (2004) 3707–3715.
[37] D.A. Gregory, Y. Zhang, P.J. Smith, X. Zhao, S.J. Ebbens, Reactive inkjet printing of biocompatible enzyme powered silk micro-rockets, Small 12 (30) (2016) 4048–4055.
[38] D.A. Gregory, P. Kumar, A. Jimenez-Franco, Y. Zhang, Y. Zhang, S.J. Ebbens, X. Zhao, Reactive inkjet printing and propulsion analysis of silk-based self-propelled micro-stirrers, JoVE 146 (2019), e59030.
[39] Y. Zhang, D.A. Gregory, Y. Zhang, P.J. Smith, S.J. Ebbens, X. Zhao, Reactive inkjet printing of functional silk stirrers for enhanced mixing and sensing, Small 15 (1) (2019) 1804213.
[40] M. Mohammed, A. Fitzpatrick, S. Malyala, I. Gibson, Customised design and development of patient specific 3D printed whole mandible implant, Proceedings of the 27th Annual International Solid Freeform Fabrication Symposium 2016, pp. 1708–1717.
[41] D.C. Ackland, D. Robinson, M. Redhead, P.V.S. Lee, A. Moskaljuk, G. Dimitroulis, A personalized 3D-printed prosthetic joint replacement for the human temporo-mandibular joint: from implant design to implantation, J. Mech. Behav. Biomed. Mater. 69 (2017) 404–411.
[42] S. Arabnejad, B. Johnston, M. Tanzer, D. Pasini, Fully porous 3D printed titanium femoral stem to reduce stress-shielding following total hip arthroplasty, J. Orthop. Res. 35 (8) (2017) 1774–1783.
[43] K. Murugesan, P.A. Anandapandian, S.K. Sharma, M. Vasantha Kumar, Comparative evaluation of dimension and surface detail accuracy of models produced by three different rapid prototype techniques, J. Indian Prosthodontic Soc. 12 (1) (2012) 16–20.
[44] M.A. Rendón-Medina, L. Andrade-Delgado, J.E. Telich-Tarriba, A. Fuente-del-Campo, C.A. Altamirano-Arcos, Dimensional error in rapid prototyping with open source software and low-cost 3D-printer, Plastic Reconst. Surg. Glob. Open 6 (1) (2018), e1646.
[45] C. Cvetkovic, R. Raman, V. Chan, B.J. Williams, M. Tolish, P. Bajaj, M.S. Sakar, H.H. Asada, M.T. Saif, R. Bashir, Three-dimensionally printed biological machines powered by skeletal muscle, Proc. Natl. Acad. Sci. U. S. A. 111 (28) (2014) 10125–10130.
[46] F. Guillemot, V. Mironov, M. Nakamura, Bioprinting is coming of age: report from the International Conference on Bioprinting and Biofabrication in Bordeaux (3B'09), Biofabrication 2 (1) (2010), 010201.
[47] J. Groll, T. Boland, T. Blunk, J.A. Burdick, D.W. Cho, P.D. Dalton, B. Derby, G. Forgacs, Q. Li, V.A. Mironov, L. Moroni, M. Nakamura, W. Shu, S. Takeuchi, G. Vozzi, T.B. Woodfield, T. Xu, J.J. Yoo, J. Malda, Biofabrication: reappraising the definition of an evolving field, Biofabrication 8 (1) (2016), 013001.
[48] L. Moroni, T. Boland, J.A. Burdick, C. De Maria, B. Derby, G. Forgacs, J. Groll, Q. Li, J. Malda, V.A. Mironov, C. Mota, M. Nakamura, W. Shu, S. Takeuchi, T.B.F. Woodfield, T. Xu, J.J. Yoo, G. Vozzi, Biofabrication: a guide to technology and terminology, Trends Biotechnol. 36 (4) (2018) 384–402.
[49] A.M. Compaan, K. Christensen, Y. Huang, Inkjet bioprinting of 3D silk fibroin cellular constructs using sacrificial alginate, ACS Biomater. Sci. Eng. 3 (8) (2017) 1519–1526.
[50] G. Gao, T. Yonezawa, K. Hubbell, G. Dai, X. Cui, Inkjet-bioprinted acrylated peptides and PEG hydrogel with human mesenchymal stem cells promote robust bone and cartilage formation with minimal printhead clogging, Biotechnol. J. 10 (10) (2015) 1568–1577.
[51] S.V. Murphy, A. Atala, 3D bioprinting of tissues and organs, Nat. Biotechnol. 32 (8) (2014) 773.
[52] A. Lee, A. Hudson, D. Shiwarski, J. Tashman, T. Hinton, S. Yerneni, J. Bliley, P. Campbell, A. Feinberg, 3D bioprinting of collagen to rebuild components of the human heart, Science 365 (6452) (2019) 482–487.
[53] A. Isaacson, S. Swioklo, C.J. Connon, 3D bioprinting of a corneal stroma equivalent, Exp. Eye Res. 173 (2018) 188–193.
[54] W.L. Ng, J.T.Z. Qi, W.Y. Yeong, M.W. Naing, Proof-of-concept: 3D bioprinting of pigmented human skin constructs, Biofabrication 10 (2) (2018), 025005.

[55] T. Xu, J. Jin, C. Gregory, J.J. Hickman, T. Boland, Inkjet printing of viable mammalian cells, Biomaterials 26 (1) (2005) 93–99.
[56] T. Xu, K.W. Binder, M.Z. Albanna, D. Dice, W. Zhao, J.J. Yoo, A. Atala, Hybrid printing of mechanically and biologically improved constructs for cartilage tissue engineering applications, Biofabrication 5 (1) (2012), 015001.
[57] X. Zhou, H. Cui, M. Nowicki, S. Miao, S.-J. Lee, F. Masood, B.T. Harris, L.G. Zhang, Three-dimensional-bioprinted dopamine-based matrix for promoting neural regeneration, ACS Appl. Mater. Interfaces 10 (10) (2018) 8993–9001.
[58] T. Boland, T. Xu, B. Damon, X. Cui, Application of inkjet printing to tissue engineering, Biotechnol. J. 1 (9) (2006) 910–917.
[59] T. Xu, W. Zhao, J.-M. Zhu, M.Z. Albanna, J.J. Yoo, A. Atala, Complex heterogeneous tissue constructs containing multiple cell types prepared by inkjet printing technology, Biomaterials 34 (1) (2013) 130–139.
[60] X.D. Hoa, A.G. Kirk, M. Tabrizian, Towards integrated and sensitive surface plasmon resonance biosensors: a review of recent progress, Biosens. Bioelectron. 23 (2) (2007) 151–160.
[61] C. Mandrycky, Z. Wang, K. Kim, D.-H. Kim, 3D bioprinting for engineering complex tissues, Biotechnol. Adv. 34 (4) (2016) 422–434.
[62] M. Albanna, K.W. Binder, S.V. Murphy, J. Kim, S.A. Qasem, W. Zhao, J. Tan, I.B. El-Amin, D.D. Dice, J. Marco, J. Green, T. Xu, A. Skardal, J.H. Holmes, J.D. Jackson, A. Atala, J.J. Yoo, In situ bioprinting of autologous skin cells accelerates wound healing of extensive excisional full-thickness wounds, Sci. Rep. 9 (1) (2019) 1856.
[63] R. Levato, T. Jungst, R.G. Scheuring, T. Blunk, J. Groll, J. Malda, From shape to function: the next step in bioprinting, Adv. Mater. 32 (2020) 1906423.
[64] A. Hasan, A. Paul, N.E. Vrana, X. Zhao, A. Memic, Y.-S. Hwang, M.R. Dokmeci, A. Khademhosseini, Microfluidic techniques for development of 3D vascularized tissue, Biomaterials 35 (26) (2014) 7308–7325.
[65] A. Morss Clyne, S. Swaminathan, A. Díaz Lantada, Biofabrication strategies for creating microvascular complexity, Biofabrication 11 (3) (2019), 032001.
[66] R.W. Barrs, J. Jia, S.E. Silver, M. Yost, Y. Mei, Biomaterials for bioprinting microvasculature, Chem. Rev. 120 (19) (2020) 10887–10949.
[67] Y. Li, X. Jiang, L. Li, Z.-N. Chen, G. Gao, R. Yao, W. Sun, 3D printing human induced pluripotent stem cells with novel hydroxypropyl chitin bioink: scalable expansion and uniform aggregation, Biofabrication 10 (4) (2018), 044101.
[68] A. Faulkner-Jones, C. Fyfe, D.-J. Cornelissen, J. Gardner, J. King, A. Courtney, W. Shu, Bioprinting of human pluripotent stem cells and their directed differentiation into hepatocyte-like cells for the generation of mini-livers in 3D, Biofabrication 7 (4) (2015), 044102.
[69] X. Ma, X. Qu, W. Zhu, Y.-S. Li, S. Yuan, H. Zhang, J. Liu, P. Wang, C.S.E. Lai, F. Zanella, G.-S. Feng, F. Sheikh, S. Chien, S. Chen, Deterministically patterned biomimetic human iPSC-derived hepatic model via rapid 3D bioprinting, Proc. Natl. Acad. Sci. 113 (8) (2016) 2206–2211.
[70] S. Jana, A. Lerman, Bioprinting a cardiac valve, Biotechnol. Adv. 33 (8) (2015) 1503–1521.
[71] E.C. Novosel, C. Kleinhans, P.J. Kluger, Vascularization is the key challenge in tissue engineering, Adv. Drug Deliv. Rev. 63 (4-5) (2011) 300–311.
[72] J. Rouwkema, B.F. Koopman, C.A.V. Blitterswijk, W.J. Dhert, J. Malda, Supply of nutrients to cells in engineered tissues, Biotechnol. Genet. Eng. Rev. 26 (1) (2009) 163–178.
[73] I.S. Kinstlinger, J.S. Miller, 3D-printed fluidic networks as vasculature for engineered tissue, Lab Chip 16 (11) (2016) 2025–2043.
[74] X. Li, L. Liu, X. Zhang, T. Xu, Research and development of 3D printed vasculature constructs, Biofabrication 10 (3) (2018), 032002.
[75] M.W. Laschke, M.D. Menger, Prevascularization in tissue engineering: current concepts and future directions, Biotechnol. Adv. 34 (2) (2016) 112–121.
[76] D. Richards, J. Jia, M. Yost, R. Markwald, Y. Mei, 3D bioprinting for vascularized tissue fabrication, Ann. Biomed. Eng. 45 (1) (2017) 132–147.
[77] S.J. Paulsen, J.S. Miller, Tissue vascularization through 3D printing: will technology bring us flow? Dev. Dyn. 244 (5) (2015) 629–640.
[78] N. Nagarajan, A. Dupret-Bories, E. Karabulut, P. Zorlutuna, N.E. Vrana, Enabling personalized implant and controllable biosystem development through 3D printing, Biotechnol. Adv. 36 (2) (2018) 521–533.
[79] J. Groll, J.A. Burdick, D.W. Cho, B. Derby, M. Gelinsky, S.C. Heilshorn, T. Jüngst, J. Malda, V.A. Mironov, K. Nakayama, A. Ovsianikov, W. Sun, S. Takeuchi, J.J. Yoo, T.B.F. Woodfield, A definition of bioinks and their distinction from biomaterial inks, Biofabrication 11 (1) (2018), 013001.
[80] M. Hospodiuk, M. Dey, D. Sosnoski, I.T. Ozbolat, The bioink: a comprehensive review on bioprintable materials, Biotechnol. Adv. 35 (2) (2017) 217–239.
[81] A.-V. Do, B. Khorsand, S.M. Geary, A.K. Salem, 3D printing of scaffolds for tissue regeneration applications, Adv. Healthc. Mater. 4 (12) (2015) 1742–1762.
[82] N. Yamamura, R. Sudo, M. Ikeda, K. Tanishita, Effects of the mechanical properties of collagen gel on the in vitro formation of microvessel networks by endothelial cells, Tissue Eng. 13 (7) (2007) 1443–1453.
[83] N. Diamantides, L. Wang, T. Pruiksma, J. Siemiatkoski, C. Dugopolski, S. Shortkroff, S. Kennedy, L.J. Bonassar, Correlating rheological properties and printability of collagen bioinks: the effects of riboflavin photocrosslinking and pH, Biofabrication 9 (3) (2017), 034102.
[84] S. Rhee, J.L. Puetzer, B.N. Mason, C.A. Reinhart-King, L.J. Bonassar, 3D bioprinting of spatially heterogeneous collagen constructs for cartilage tissue engineering, ACS Biomater. Sci. Eng. 2 (10) (2016) 1800–1805.
[85] J. Lee, M. Yeo, W. Kim, Y. Koo, G.H. Kim, Development of a tannic acid cross-linking process for obtaining 3D porous cell-laden collagen structure, Int. J. Biol. Macromol. 110 (2018) 497–503.
[86] W. Kim, G. Kim, Intestinal villi model with blood capillaries fabricated using collagen-based bioink and dual-cell-printing process, ACS Appl. Mater. Interfaces 10 (48) (2018) 41185–41196.
[87] Q. Gao, X. Niu, L. Shao, L. Zhou, Z. Lin, A. Sun, J. Fu, Z. Chen, J. Hu, Y. Liu, Y. He, 3D printing of complex GelMA-based scaffolds with nanoclay, Biofabrication 11 (3) (2019), 035006.
[88] Q. Chen, X. Tian, J. Fan, H. Tong, Q. Ao, X. Wang, An interpenetrating alginate/gelatin network for three-dimensional (3D) cell cultures and organ bioprinting, Molecules 25 (3) (2020) 756.
[89] L. Shao, Q. Gao, C. Xie, J. Fu, M. Xiang, Z. Liu, L. Xiang, Y. He, Sacrificial microgel-laden bioink-enabled 3D bioprinting of mesoscale pore networks, Bio-Design Manufact. 3 (1) (2020) 30–39.
[90] L. Shao, Q. Gao, C. Xie, J. Fu, M. Xiang, Y. He, Synchronous 3D bioprinting of large-scale cell-laden constructs with nutrient networks, Adv. Healthc. Mater. 9 (2019) 1901142.
[91] P.S. Gungor-Ozkerim, I. Inci, Y.S. Zhang, A. Khademhosseini, M.R. Dokmeci, Bioinks for 3D bioprinting: an overview, Biomater. Sci. 6 (5) (2018) 915–946.
[92] J. Jang, H.-J. Park, S.-W. Kim, H. Kim, J.Y. Park, S.J. Na, H.J. Kim, M.N. Park, S.H. Choi, S.H. Park, S.W. Kim, S.-M. Kwon, P.-J. Kim, D.-W. Cho, 3D printed complex tissue construct using stem cell-laden decellularized extracellular matrix bioinks for cardiac repair, Biomaterials 112 (2017) 264–274.
[93] P.A. Mollica, E.N. Booth-Creech, J.A. Reid, M. Zamponi, S.M. Sullivan, X.-L. Palmer, P.C. Sachs, R.D. Bruno, 3D bioprinted mammary organoids and tumoroids in human mammary derived ECM hydrogels, Acta Biomater. 95 (2019) 201–213.
[94] G. Gao, J.H. Lee, J. Jang, D.H. Lee, J.-S. Kong, B.S. Kim, Y.-J. Choi, W.B. Jang, Y.J. Hong, S.-M. Kwon, D.-W. Cho, Tissue engineered bio-blood-vessels constructed using a tissue-specific bioink and 3D coaxial cell printing technique: a novel therapy for ischemic disease, Adv. Funct. Mater. 27 (33) (2017) 1700798.
[95] M. Ali, P.R. Anil Kumar, James J. Yoo, Faten Zahran, Anthony Atala, Sang Jin Lee, A photo-crosslinkable kidney ECM-derived bioink accelerates renal tissue formation, Adv. Healthc. Mater. 8 (7) (2019) 1800992.
[96] A. Skardal, M. Devarasetty, H.-W. Kang, I. Mead, C. Bishop, T. Shupe, S.J. Lee, J. Jackson, J. Yoo, S. Soker, A. Atala, A hydrogel bioink toolkit for mimicking native tissue biochemical and mechanical properties in bioprinted tissue constructs, Acta Biomater. 25 (2015) 24–34.
[97] K. Narayanan, K.-J. Leck, S. Gao, A.C. Wan, Three-dimensional reconstituted extracellular matrix scaffolds for tissue engineering, Biomaterials 30 (26) (2009) 4309–4317.
[98] N. Noor, A. Shapira, R. Edri, I. Gal, L. Wertheim, T. Dvir, 3D printing of personalized thick and perfusable cardiac patches and hearts, Adv. Sci. 6 (11) (2019) 1900344.
[99] J.M. Edgar, M. Robinson, S.M. Willerth, Fibrin hydrogels induce mixed dorsal/ventral spinal neuron identities during differentiation of human induced pluripotent stem cells, Acta Biomater. 51 (2017) 237–245.
[100] M. Robinson, S. Douglas, S.M. Willerth, Mechanically stable fibrin scaffolds promote viability and induce neurite outgrowth in neural aggregates derived from human induced pluripotent stem cells, Sci. Rep. 7 (1) (2017) 6250.
[101] X. Dong, X. Lu, K. Kingston, E. Brewer, B.A. Juliar, O.D. Kripfgans, J.B. Fowlkes, R.T. Franceschi, A.J. Putnam, Z. Liu, M.L. Fabiilli, Controlled delivery of basic fibroblast growth factor (bFGF) using acoustic droplet vaporization stimulates endothelial network formation, Acta Biomater. 97 (2019) 409–419.
[102] N. Zhao, A. Suzuki, X. Zhang, P. Shi, L. Abune, J. Coyne, H. Jia, N. Xiong, G. Zhang, Y. Wang, Dual aptamer-functionalized in situ injectable fibrin hydrogel for promotion of angiogenesis via codelivery of vascular endothelial growth factor and platelet-derived growth factor-BB, ACS Appl. Mater. Interfaces 11 (20) (2019) 18123–18132.
[103] K.C. Murphy, J. Whitehead, D. Zhou, S.S. Ho, J.K. Leach, Engineering fibrin hydrogels to promote the wound healing potential of mesenchymal stem cell spheroids, Acta Biomater. 64 (2017) 176–186.
[104] S. Ji, M. Guvendiren, recent advances in bioink design for 3D bioprinting of tissues and organs, Front. Bioeng. Biotechnol. 5 (2017) 23.
[105] L.J. Currie, J.R. Sharpe, R. Martin, The use of fibrin glue in skin grafts and tissue-engineered skin replacements, Plast. Reconstr. Surg. 108 (2001) 1713–1726.
[106] T.H. Jovic, G. Kungwengwe, A. Mills, I.S. Whitaker, Plant-derived biomaterials: a review of 3D bioprinting and biomedical applications, Front. Mech. Eng. 5 (2019) 19.
[107] B.J. de Gans, P.C. Duineveld, U.S. Schubert, Inkjet printing of polymers: state of the art and future developments, Adv. Mater. 16 (3) (2004) 203–213.
[108] Y. Wang, X. Huang, Y. Shen, R. Hang, X. Zhang, Y. Wang, X. Yao, B. Tang, Direct writing alginate bioink inside pre-polymers of hydrogels to create patterned vascular networks, J. Mater. Sci. 54 (10) (2019) 7883–7892.
[109] K.Y. Lee, D.J. Mooney, Alginate: properties and biomedical applications, Prog. Polym. Sci. 37 (1) (2012) 106–126.
[110] L. Benning, L. Gutzweiler, K. Tröndle, J. Riba, R. Zengerle, P. Koltay, S. Zimmermann, G.B. Stark, G. Finkenzeller, Assessment of hydrogels for bioprinting of endothelial cells, J. Biomed. Mater. Res. A 106 (4) (2018) 935–947.
[111] P. Rastogi, B. Kandasubramanian, Review of alginate-based hydrogel bioprinting for application in tissue engineering, Biofabrication 11 (4) (2019), 042001.
[112] M.D. Sarker, S. Naghieh, A.D. McInnes, L. Ning, D.J. Schreyer, X. Chen, Biofabrication of peptide-modified alginate scaffolds: printability, mechanical stability and neurite outgrowth assessments, Bioprinting 14 (2019), e00045.
[113] R. Xie, W. Zheng, L. Guan, Y. Ai, Q. Liang, Engineering of hydrogel materials with perfusable microchannels for building vascularized tissues, Small 16 (15) (2020) 1902838.
[114] A. Skardal, J. Zhang, G.D. Prestwich, Bioprinting vessel-like constructs using hyaluronan hydrogels crosslinked with tetrahedral polyethylene glycol tetracrylates, Biomaterials 31 (24) (2010) 6173–6181.
[115] W. Jia, P.S. Gungor-Ozkerim, Y.S. Zhang, K. Yue, K. Zhu, W. Liu, Q. Pi, B. Byambaa, M.R. Dokmeci, S.R. Shin, A. Khademhosseini, Direct 3D bioprinting of perfusable vascular constructs using a blend bioink, Biomaterials 106 (2016) 58–68.

[116] D.B. Kolesky, K.A. Homan, M.A. Skylar-Scott, J.A. Lewis, Three-dimensional bioprinting of thick vascularized tissues, Proc. Natl. Acad. Sci. 113 (12) (2016) 3179.
[117] S.C. Millik, A.M. Dostie, D.G. Karis, P.T. Smith, M. McKenna, N. Chan, C.D. Curtis, E. Nance, A.B. Theberge, A. Nelson, 3D printed coaxial nozzles for the extrusion of hydrogel tubes toward modeling vascular endothelium, Biofabrication 11 (4) (2019), 045009.
[118] A. Jacoby, K.A. Morrison, R.C. Hooper, O. Asanbe, J. Joyce, R. Bleecker, R.H. Weinreb, H.L. Osoria, S. Mukherjee, J.A. Spector, Fabrication of capillary-like structures with Pluronic F127® and Kerria lacca resin (shellac) in biocompatible tissue-engineered constructs, J. Tissue Eng. Regen. Med. 11 (8) (2017) 2388–2397.
[119] P.J. Smith, A. Morrin, Reactive inkjet printing, J. Mater. Chem. 22 (22) (2012) 10965–10970.
[120] K. Christensen, C. Xu, W. Chai, Z. Zhang, J. Fu, Y. Huang, Freeform inkjet printing of cellular structures with bifurcations, Biotechnol. Bioeng. 112 (5) (2015) 1047–1055.
[121] C. Tse, R. Whiteley, T. Yu, J. Stringer, S. MacNeil, J.W. Haycock, P.J. Smith, Inkjet printing Schwann cells and neuronal analogue NG108-15 cells, Biofabrication 8 (1) (2016), 015017.
[122] D. Lee, D. Lee, Y. Won, H. Hong, Y. Kim, H. Song, J.C. Pyun, Y.S. Cho, W. Ryu, J. Moon, Insertion of vertically aligned nanowires into living cells by inkjet printing of cells, Small 12 (11) (2016) 1446–1457.
[123] C.X. Xu, W.X. Chai, Y. Huang, R.R. Markwald, Scaffold-free inkjet printing of three-dimensional zigzag cellular tubes, Biotechnol. Bioeng. 109 (12) (2012) 3152–3160.
[124] S.V. Murphy, A. Atala, 3D bioprinting of tissues and organs, Nat. Biotechnol. 32 (8) (2014) 773–785.
[125] H. Gudapati, M. Dey, I. Ozbolat, A comprehensive review on droplet-based bioprinting: past, present and future, Biomaterials 102 (2016) 20–42.
[126] J.A. Phillippi, E. Miller, L. Weiss, J. Huard, A. Waggoner, P. Campbell, Microenvironments engineered by inkjet bioprinting spatially direct adult stem cells toward muscle- and bone-like subpopulations, Stem Cells 26 (1) (2008) 127–134.
[127] X. Li, B. Liu, B. Pei, J. Chen, D. Zhou, J. Peng, X. Zhang, W. Jia, T. Xu, Inkjet bioprinting of biomaterials, Chem. Rev. 120 (19) (2020) 10793–10833.
[128] X. Li, X. Wang, H. Chen, Z. Jin, X. Dai, X. Zhang, L. Zhang, T. Xu, A comparative study of the behavior of neural progenitor cells in extrusion-based in vitro hydrogel models, Biomed. Mater. 14 (6) (2019), 065001.
[129] T. Liu, Y. Pang, Z. Zhou, R. Yao, W. Sun, An integrated cell printing system for the construction of heterogeneous tissue models, Acta Biomater. 95 (2019) 245–257.
[130] L. Ruiz-Cantu, A. Gleadall, C. Faris, J. Segal, K. Shakesheff, J. Yang, Multi-material 3D bioprinting of porous constructs for cartilage regeneration, Mater. Sci. Eng. C 109 (2020) 110578.
[131] W. Sun, B. Starly, A.C. Daly, J.A. Burdick, J. Groll, G. Skeldon, W. Shu, Y. Sakai, M. Shinohara, M. Nishikawa, J. Jang, D.-W. Cho, M. Nie, S. Takeuchi, S. Ostrovidov, A. Khademhosseini, R.D. Kamm, V. Mironov, L. Moroni, I.T. Ozbolat, The bioprinting roadmap, Biofabrication 12 (2) (2020), 022002.
[132] A.K. Miri, A. Khalilpour, B. Cecen, S. Maharjan, S.R. Shin, A. Khademhosseini, Multiscale bioprinting of vascularized models, Biomaterials 198 (2019) 204–216.
[133] J. Malda, J. Visser, F.P. Melchels, T. Jungst, W.E. Hennink, W.J. Dhert, J. Groll, D.W. Hutmacher, 25th anniversary article: engineering hydrogels for biofabrication, Adv. Mater. 25 (36) (2013) 5011–5028.
[134] D.B. Kolesky, R.L. Truby, A.S. Gladman, T.A. Busbee, K.A. Homan, J.A. Lewis, 3D bioprinting of vascularized, heterogeneous cell-laden tissue constructs, Adv. Mater. 26 (19) (2014) 3124–3130.
[135] J.K. Placone, A.J. Engler, Recent advances in extrusion-based 3D printing for biomedical applications, Adv. Healthc. Mater. 7 (8) (2018) 1701161.
[136] V.K. Lee, D.Y. Kim, H. Ngo, Y. Lee, L. Seo, S.-S. Yoo, P.A. Vincent, G. Dai, Creating perfused functional vascular channels using 3D bio-printing technology, Biomaterials 35 (28) (2014) 8092–8102.
[137] M.J. Rodriguez, J. Brown, J. Giordano, S.J. Lin, F.G. Omenetto, D.L. Kaplan, Silk based bioinks for soft tissue reconstruction using 3-dimensional (3D) printing with in vitro and in vivo assessments, Biomaterials 117 (2017) 105–115.
[138] K. Markstedt, A. Mantas, I. Tournier, H. Martinez Avila, D. Hagg, P. Gatenholm, 3D bioprinting human chondrocytes with nanocellulose-alginate bioink for cartilage tissue engineering applications, Biomacromolecules 16 (5) (2015) 1489–1496.
[139] M.A. Skylar-Scott, S.G. Uzel, L.L. Nam, J.H. Ahrens, R.L. Truby, S. Damaraju, J.A. Lewis, Biomanufacturing of organ-specific tissues with high cellular density and embedded vascular channels, Sci. Adv. 5 (9) (2019), eaaw2459.
[140] Q. Gao, Y. He, J.-z. Fu, A. Liu, L. Ma, Coaxial nozzle-assisted 3D bioprinting with built-in microchannels for nutrients delivery, Biomaterials 61 (2015) 203–215.
[141] X. Wang, X. Li, X. Dai, X. Zhang, J. Zhang, T. Xu, Q. Lan, Coaxial extrusion bioprinted shell-core hydrogel microfibers mimic glioma microenvironment and enhance the drug resistance of cancer cells, Colloids Surf. B: Biointerfaces 171 (2018) 291–299.
[142] Xingliang Dai, Libiao Liu, Jia Ouyang, Xinda Li, Xinzhi Zhang, Qing Lan, T. Xu, Coaxial 3D bioprinting of self-assembled multicellular heterogeneous tumor fibers, Sci. Rep. 7 (2017) 1457.
[143] W. Zhang, C. Feng, G. Yang, G. Li, X. Ding, S. Wang, Y. Dou, Z. Zhang, J. Chang, C. Wu, X. Jiang, 3D-printed scaffolds with synergistic effect of hollow-pipe structure and bioactive ions for vascularized bone regeneration, Biomaterials 135 (2017) 85–95.
[144] Q. Gao, Z. Liu, Z. Lin, J. Qiu, Y. Liu, A. Liu, Y. Wang, M. Xiang, B. Chen, J. Fu, 3D bioprinting of vessel-like structures with multilevel fluidic channels, ACS Biomaterial. Sci. Eng. 3 (3) (2017) 399–408.
[145] H. Cui, W. Zhu, Y. Huang, C. Liu, Z.-X. Yu, M. Nowicki, S. Miao, Y. Cheng, X. Zhou, S.-J. Lee, Y. Zhou, S. Wang, M. Mohiuddin, K. Horvath, L.G. Zhang, In vitro and in vivo evaluation of 3D bioprinted small-diameter vasculature with smooth muscle and endothelium, Biofabrication 12 (1) (2019), 015004.
[146] G. Gao, H. Kim, B.S. Kim, J.S. Kong, J.Y. Lee, B.W. Park, S. Chae, J. Kim, K. Ban, J. Jang, H.-J. Park, D.-W. Cho, Tissue-engineering of vascular grafts containing endothelium and smooth-muscle using triple-coaxial cell printing, Appl. Phys. Rev. 6 (4) (2019), 041402.
[147] D. Kang, G. Hong, S. An, I. Jang, W.S. Yun, J.H. Shim, S. Jin, Bioprinting of multiscaled hepatic lobules within a highly vascularized construct, Small 16 (2020) 1905505.
[148] X. Wang, X. Li, J. Ding, X. Long, H. Zhang, X. Zhang, X. Jiang, T. Xu, 3D bioprinted glioma microenvironment for glioma vascularization, J. Biomed. Mater. Res. Part A (2020) 1–11.
[149] J.S. Miller, K.R. Stevens, M.T. Yang, B.M. Baker, D.-H.T. Nguyen, D.M. Cohen, E. Toro, A.A. Chen, P.A. Galie, X. Yu, Rapid casting of patterned vascular networks for perfusable engineered three-dimensional tissues, Nat. Mater. 11 (9) (2012) 768–774.
[150] R. Pimentel, S.K. Ko, C. Caviglia, A. Wolff, J. Emnéus, S.S. Keller, M. Dufva, Three-dimensional fabrication of thick and densely populated soft constructs with complex and actively perfused channel network, Acta Biomater. 65 (2018) 174–184.
[151] Y. Lu, G. Mapili, G. Suhali, S. Chen, K. Roy, A digital micro-mirror device-based system for the microfabrication of complex, spatially patterned tissue engineering scaffolds, J. Biomed. Mater. Res. A 77A (2) (2006) 396–405.
[152] J.R. Tumbleston, D. Shirvanyants, N. Ermoshkin, R. Janusziewicz, A.R. Johnson, D. Kelly, K. Chen, R. Pinschmidt, J.P. Rolland, A. Ermoshkin, Continuous liquid interface production of 3D objects, Science 347 (6228) (2015) 1349–1352.
[153] H. Cui, T. Esworthy, X. Zhou, S.Y. Hann, R.I. Glazer, R. Li, L.G. Zhang, Engineering a novel 3D printed vascularized tissue model for investigating breast cancer metastasis to bone, Adv. Healthc. Mater. 9 (2019) 1900924.
[154] B. Grigoryan, S.J. Paulsen, D.C. Corbett, D.W. Sazer, C.L. Fortin, A.J. Zaita, P.T. Greenfield, N.J. Calafat, J.P. Gounley, A.H. Ta, Multivascular networks and functional intravascular topologies within biocompatible hydrogels, Science 364 (6439) (2019) 458–464.
[155] R. Zhang, N.B. Larsen, Stereolithographic hydrogel printing of 3D culture chips with biofunctionalized complex 3D perfusion networks, Lab Chip 17 (24) (2017) 4273–4282.
[156] F. Guillemot, A. Souquet, S. Catros, B. Guillotin, J. Lopez, M. Faucon, B. Pippenger, R. Bareille, M. Rémy, S. Bellance, High-throughput laser printing of cells and biomaterials for tissue engineering, Acta Biomater. 6 (7) (2010) 2494–2500.
[157] J. Fernández-Pradas, C. Florian, F. Caballero-Lucas, P. Sopeña, J. Morenza, P. Serra, Laser-induced forward transfer: propelling liquids with light, Appl. Surf. Sci. 418 (2017) 559–564.
[158] S. Catros, B. Guillotin, M. Bačáková, J.-C. Fricain, F. Guillemot, Effect of laser energy, substrate film thickness and bioink viscosity on viability of endothelial cells printed by Laser-Assisted Bioprinting, Appl. Surf. Sci. 257 (12) (2011) 5142–5147.
[159] R. Xiong, Z. Zhang, W. Chai, Y. Huang, D.B. Chrisey, Freeform drop-on-demand laser printing of 3D alginate and cellular constructs, Biofabrication 7 (4) (2015), 045011.
[160] C. Tomasina, T. Bodet, C. Mota, L. Moroni, S. Camarero-Espinosa, Bioprinting vasculature: materials, cells and emergent techniques, Materials 12 (17) (2019) 2701.
[161] J. Yan, Y. Huang, D.B. Chrisey, Laser-assisted printing of alginate long tubes and annular constructs, Biofabrication 5 (1) (2012), 015002.
[162] Y.C. Li, Y.S. Zhang, A. Akpek, S.R. Shin, A. Khademhosseini, 4D bioprinting: the next-generation technology for biofabrication enabled by stimuli-responsive materials, Biofabrication 9 (1) (2016), 012001.